Stellar Atmospheres and Surfaces

Jason Aufdenberg
Michelson Postdoctoral Fellow
National Optical Astronomy Observatory

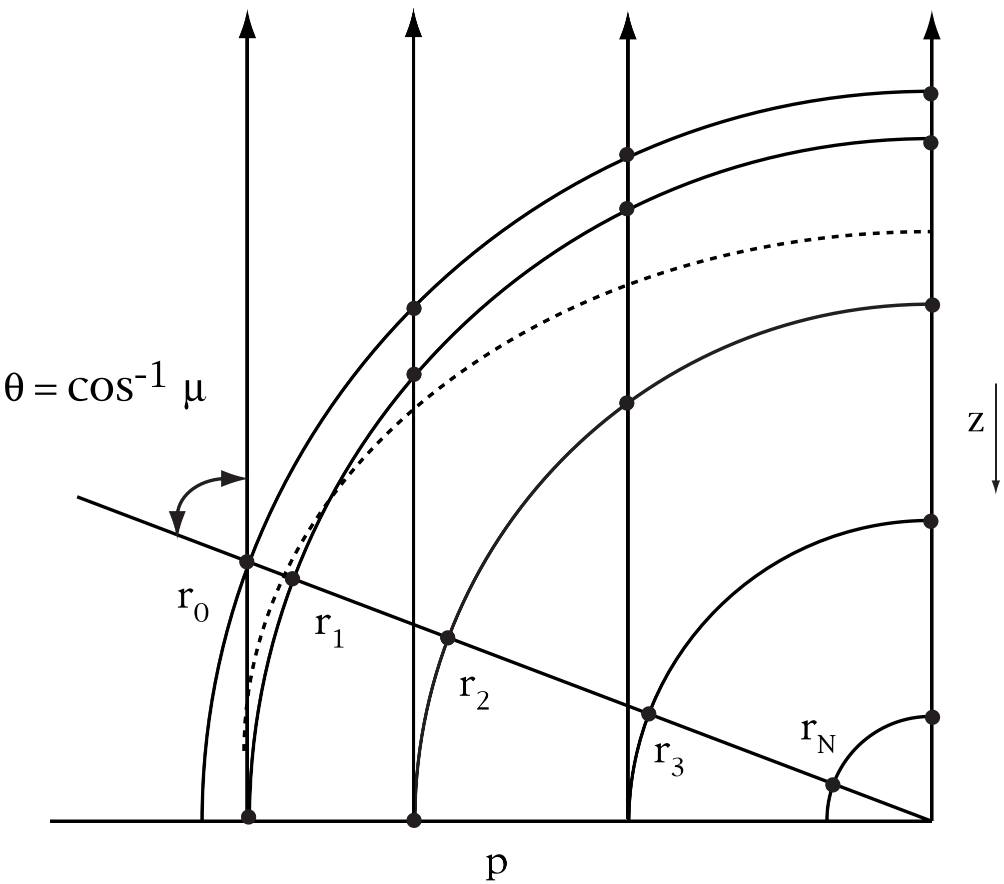

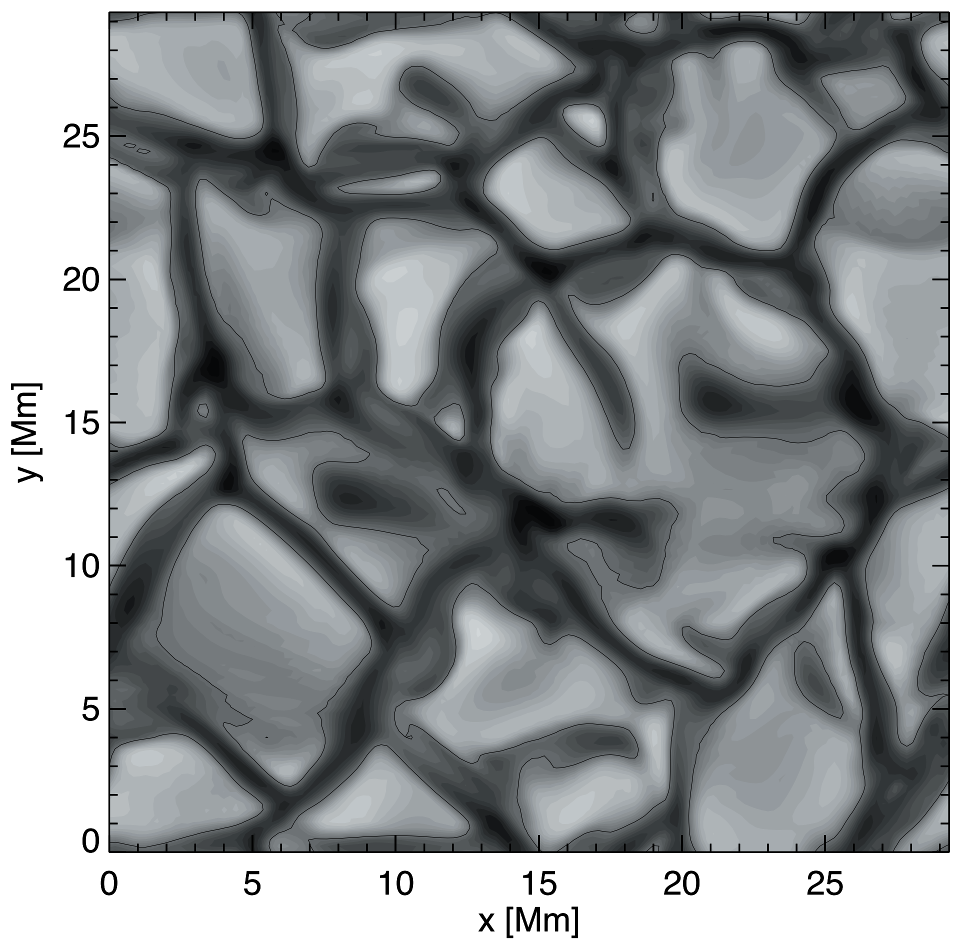

What's to Come....

- A Close Look at.....
  Limb Darkening,
  Plane-Parallel Models,
  The Sun,
  Granulation and 3-D Models,
  and Procyon

- Extended Photospheres:
  Lines and Molecular Bands
  Spherical vs. Plane-Parallel Limb Darkening
  Rosseland Angular Diameter

- Odds and Ends:
  Gravity Darkening vs. Limb Darkening
  Stars are not Blackbodies
  Synthetic Visibilities
  Stellar Surfaces for the Future

For the best spatial resolution...
Get to know our Sun!

Reconstructing the Sun's Temperature Structure: Spatially Resolved *Absolute* Intensities

$$T_b^{\,\mathrm{center}} = \frac{14388}{\lambda \ln\left[(11909/\lambda^5 I_\lambda) + 1\right]}$$

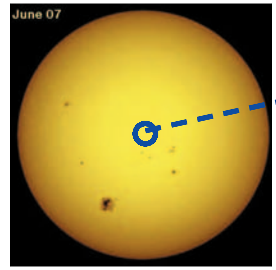

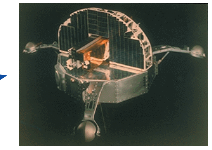

Orbiting Solar Observatory 6

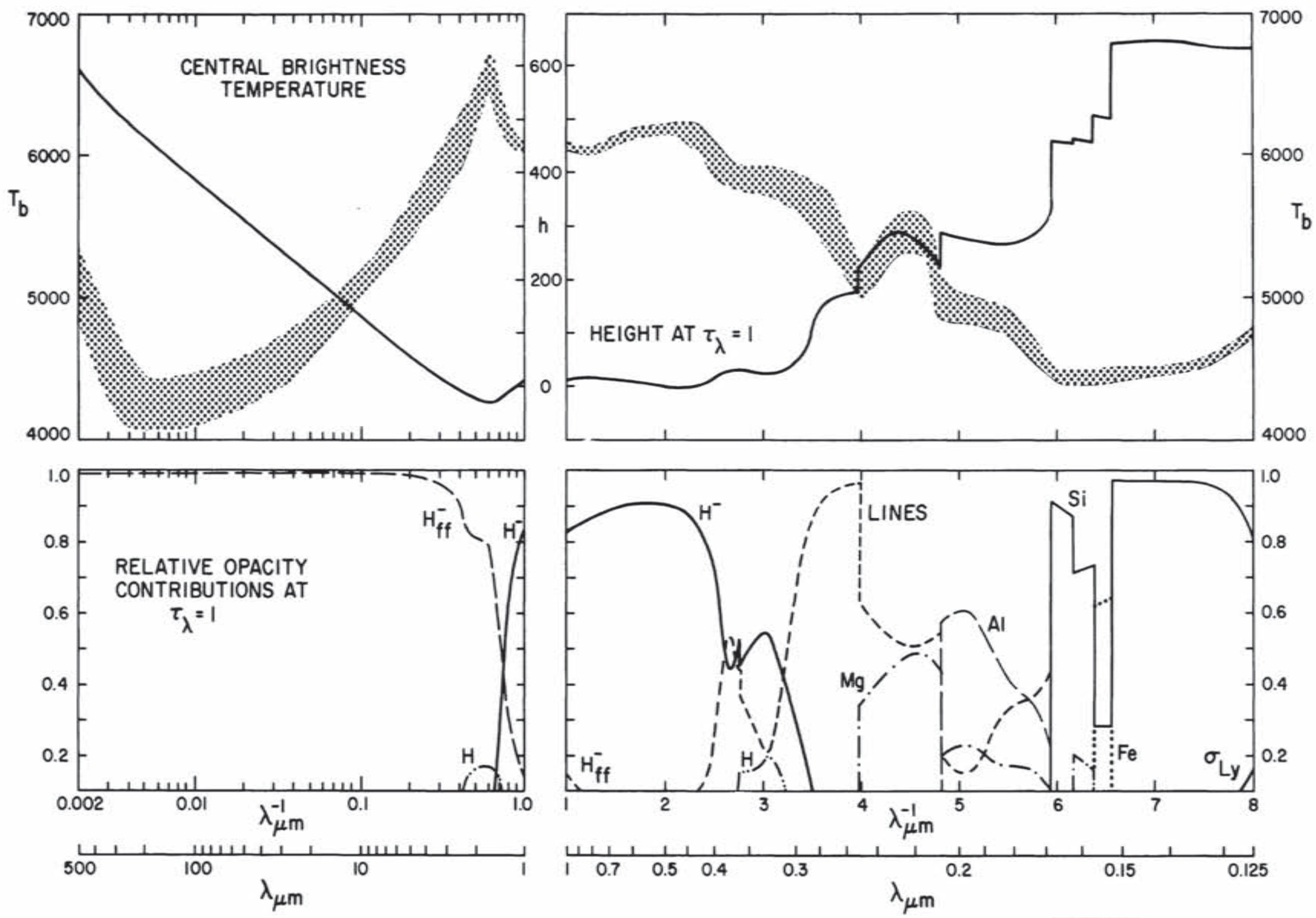

Vernezza, Avrett, & Loeser (1976) ApJS 30, 1

If spatial resolution is not an issue:
Measure the intensity, I_λ, in absolute units at the center of the Sun's disk and solve for the brightness temperature, T_b.

This won't work for other stars (at least not yet!).

Limb Darkening - Probing Atmospheric Structure

<u>If you measure:</u>

•The diameter of a star at two or more wavelengths

•The amplitude of the 2nd (or higher) lobe of a star's visibility curve at one or more wavelengths

You are likely measuring a temperature gradient in (and possibly on) the star's atmosphere.

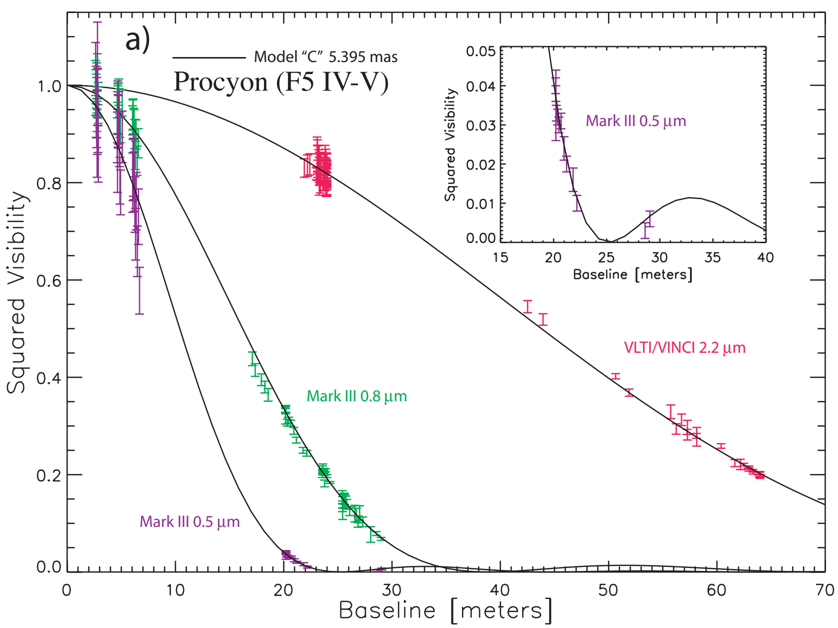

Aufdenberg, Ludwig, Kervella (2005) ApJ 633, 424

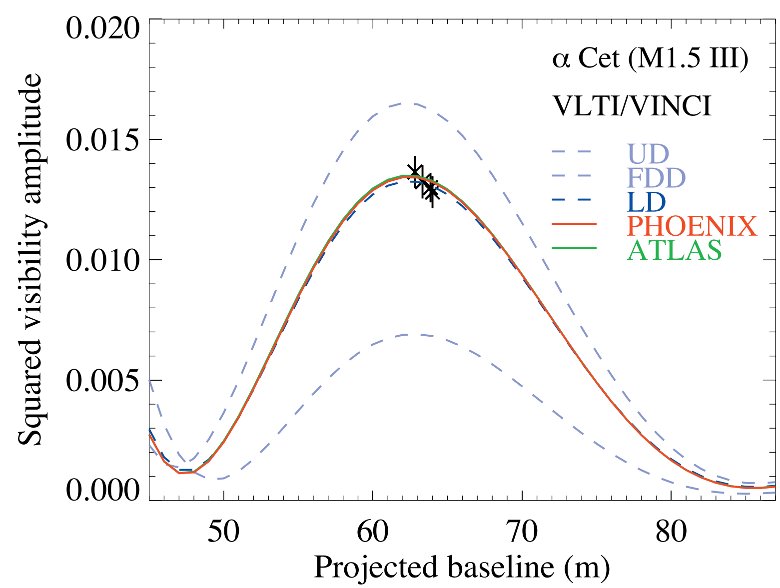

Wittkowski et al. (2006b) A&A, submitted

Limb Darkening Basics I

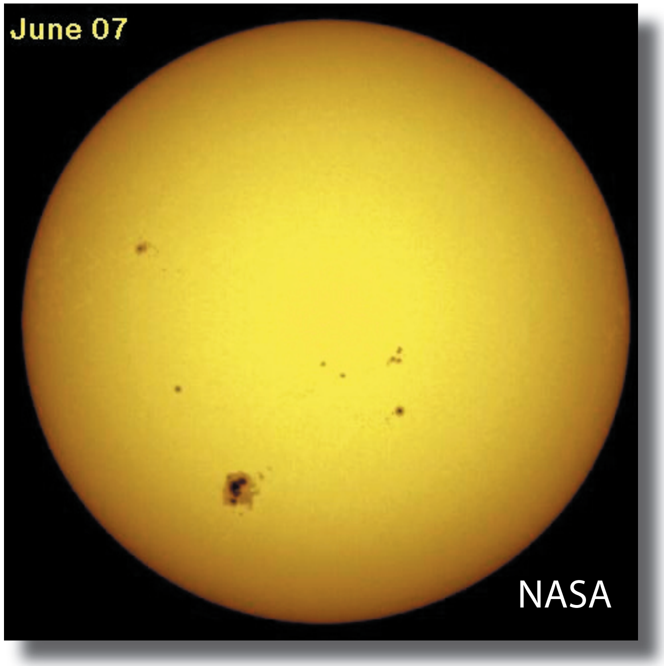

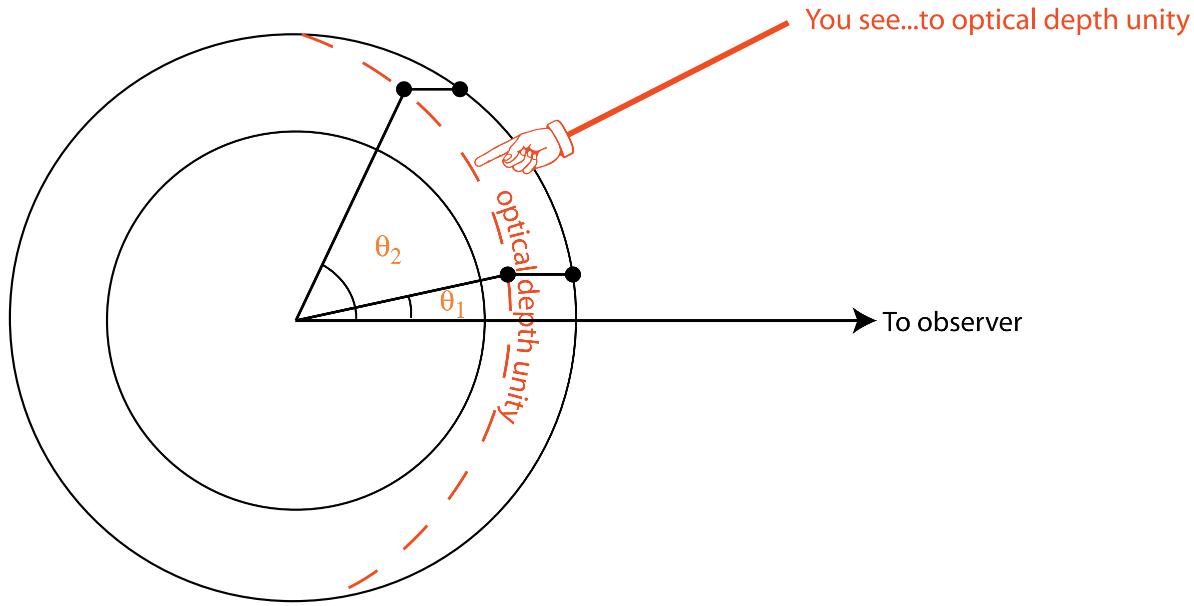

(a) Deeper, hotter layers are visible near the disk center

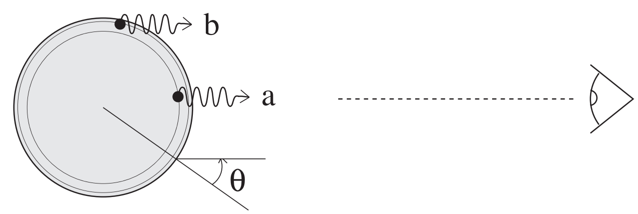

(b) Shallower, cooler layers are visible near the disk limb

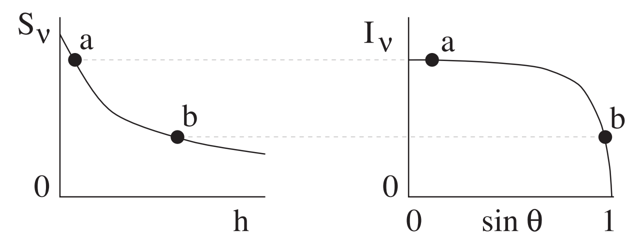

source function as a function of depth

center to limb intensity profile

isothermal atmospheres do not exhibit limb darkening

A Plane Parallel Atmosphere

Center-to-limb intensity profile derived from a series of slanted views into a plane parallel atmosphere

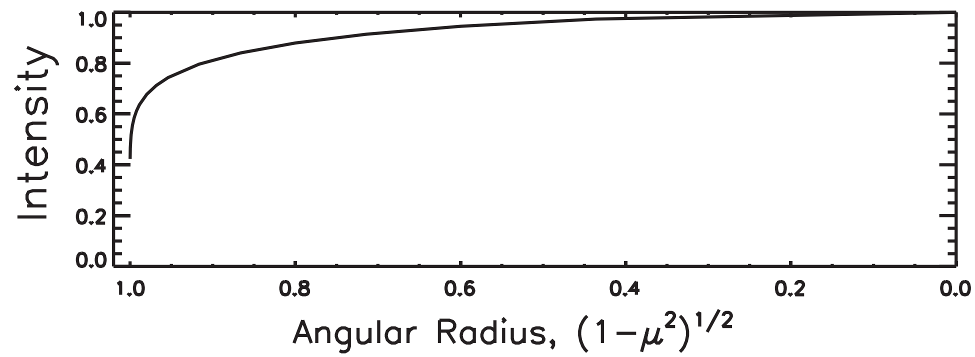

0.1% of stellar radius

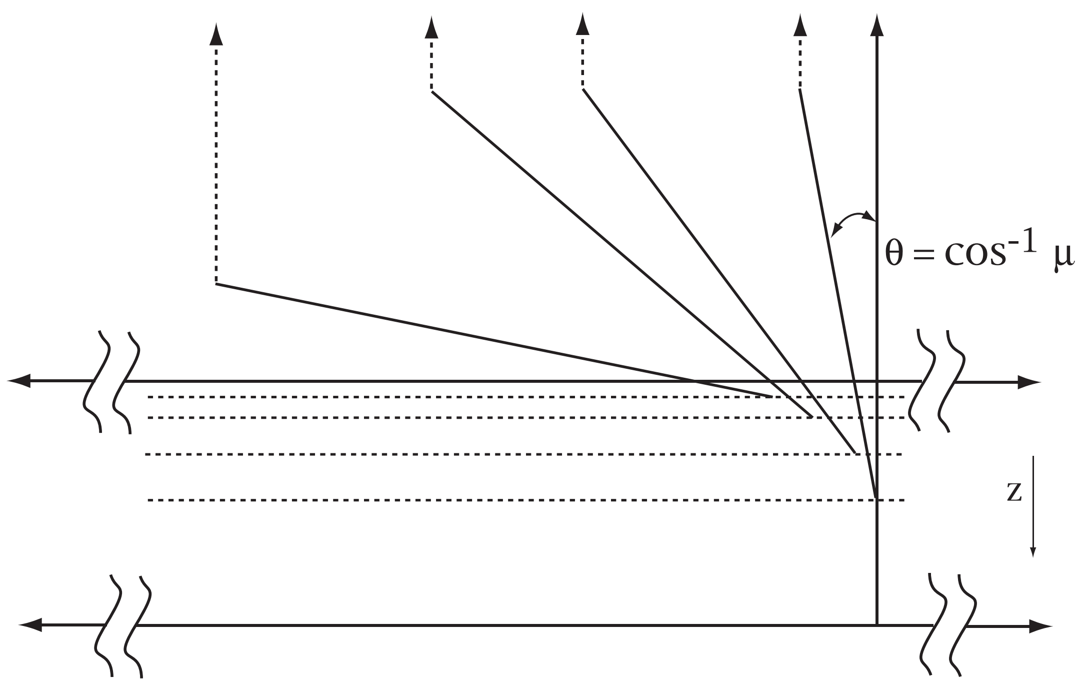

Limb Darkening Basics II

Continuum wavelength dependence

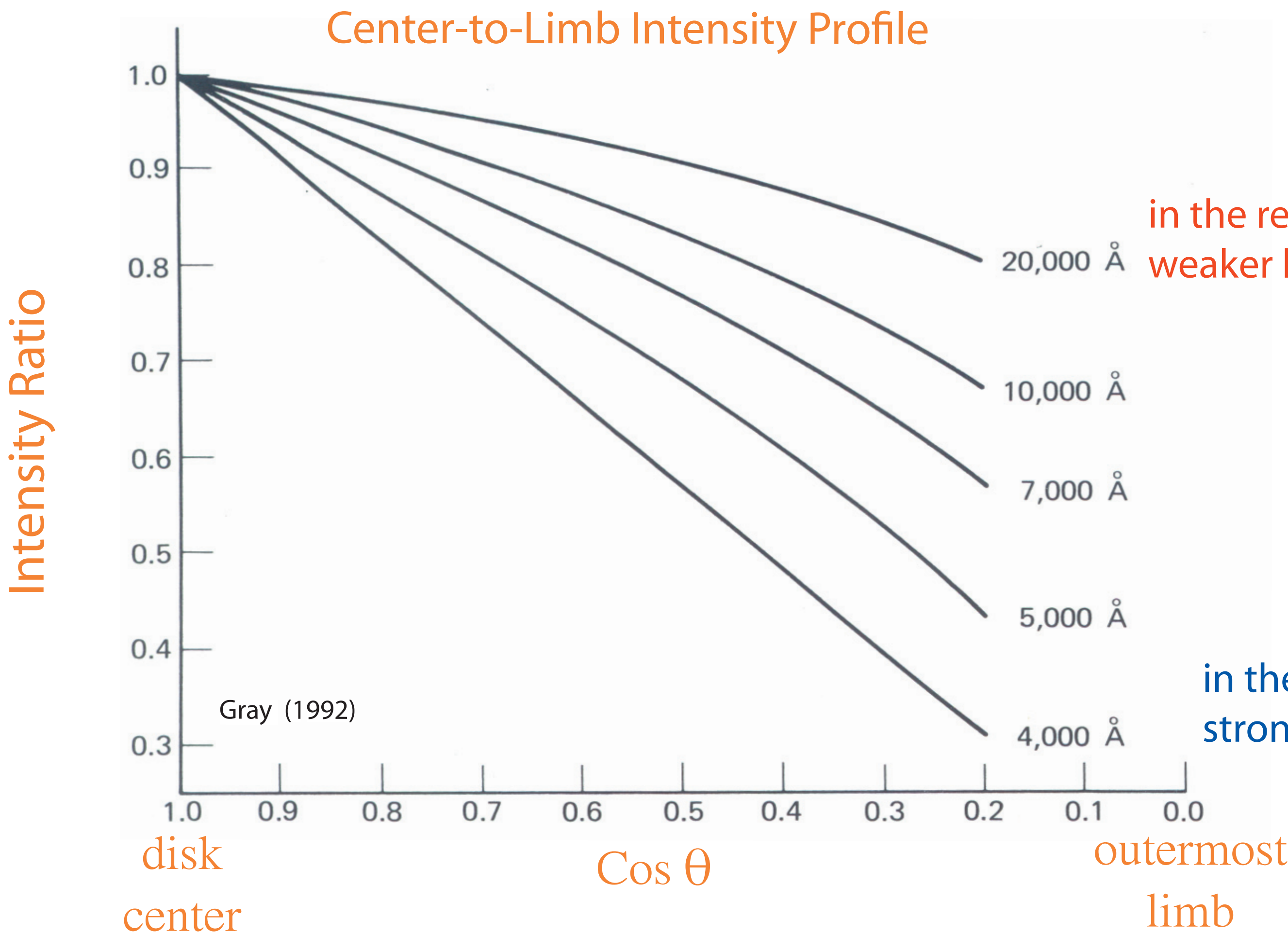

in the red:
weaker limb darkening

in the blue:
stronger limb darkening

$$B_\lambda \approx \frac{2ckT}{\lambda^4} \quad \text{when } hc \ll k\lambda T$$

Rayleigh-Jeans approx. of the Planck function

$$\frac{d\,B_\lambda}{d\,T} \approx \frac{2ck}{\lambda^4}$$

The change in intensity with temperature increases with decreasing wavelength

Early Observations of Solar Limb Darkening

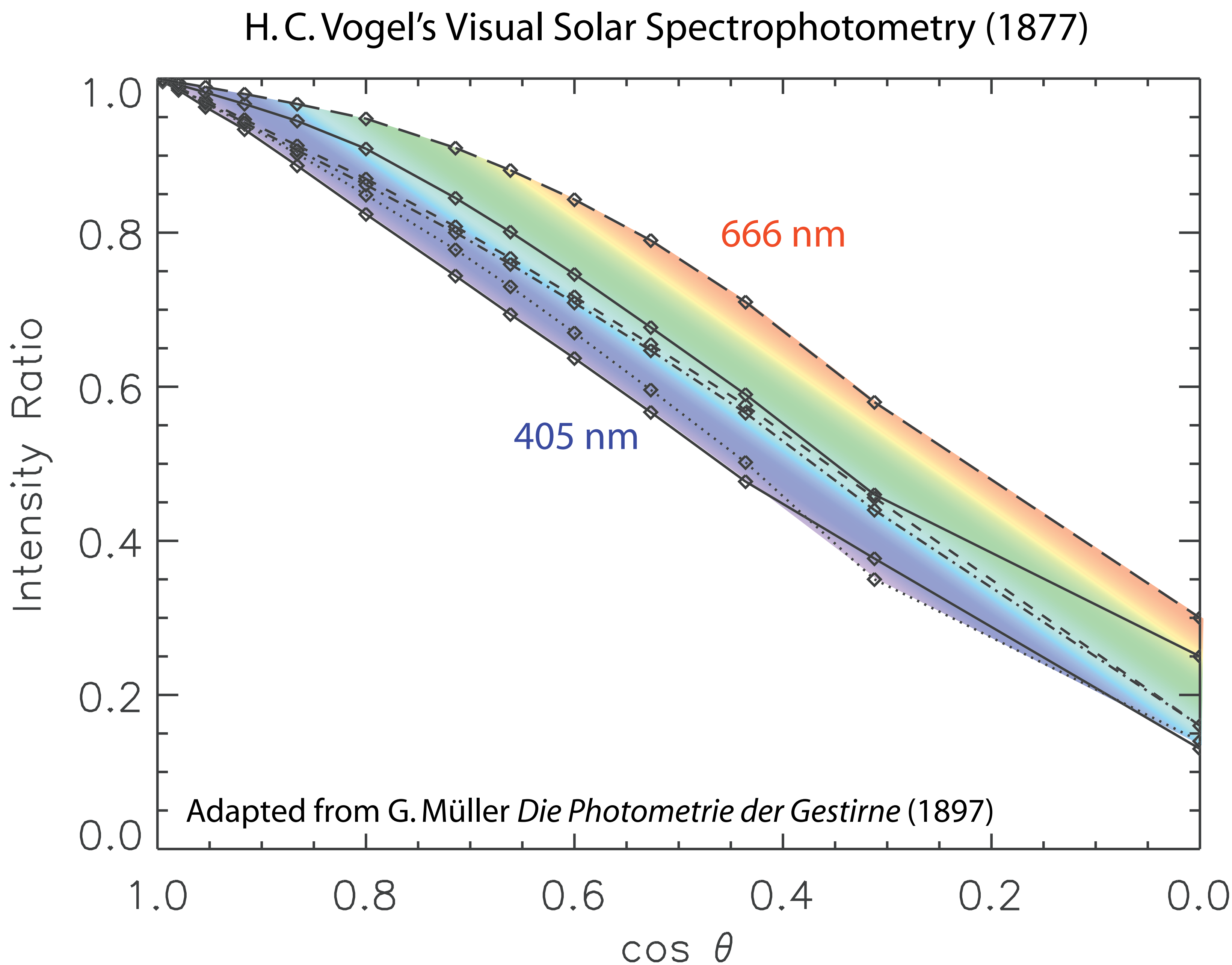

Early Model Limb Darkening

1906 - K. Schwarzschild
Derived a center-to-limb profile for the Sun with a radiative equilibrium temperature structure. He showed this to be consistent with observations, ruling out an adiabatic equilibrium temperature structure.

Schwarzschild (1906) Models vs. Contemporary Data

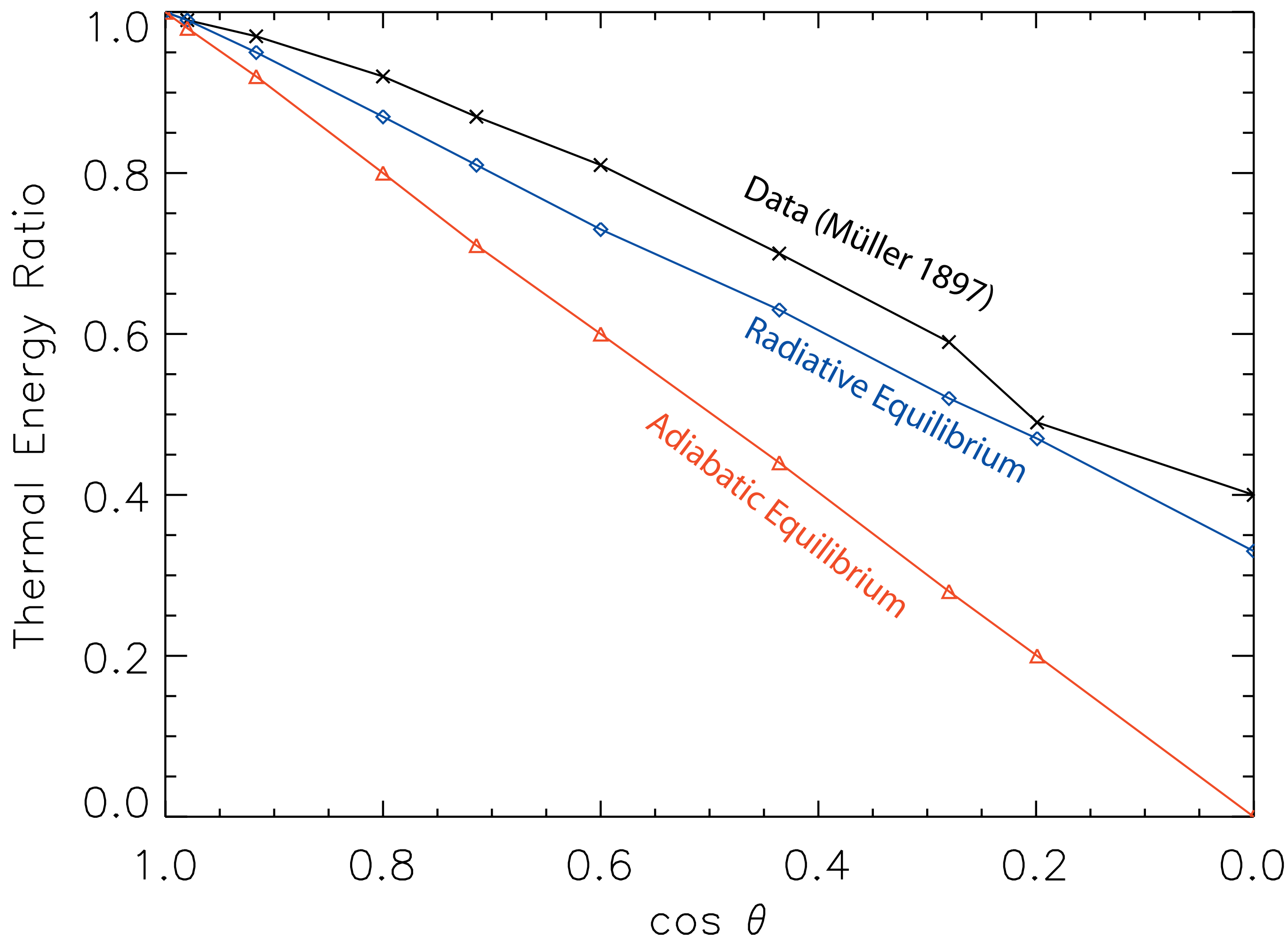

Adapted from K. Schwarzschild (1906) "Über das Gleichgewicht der Sonnenatmosphäre"
Nachrichten von der Königlichen Gesellschaft der Wissenschaften zu Göttingen. Math.-phys. Kalsse, 295, 41
See translation in D. H. Menzel, Ed., *Selected Papers on the Transfer of Radiation* (1966) NY: Dover

Limb Darkening Basics II

Linking intensity to depth: the transfer equation

The *formal solution* to the plane parallel transfer equation:

$$I_\nu^+(\tau_\nu = 0, \mu) = \int_0^\infty S_\nu(t_\nu)\, \mathrm{e}^{-t_\nu/\mu}\, \mathrm{d}t_\nu/\mu.$$

The outgoing intensity $\mathbf{I}_\nu$ at the surface at the atmosphere (optical depth $\boldsymbol{\tau}_\nu$ = **0**) is the integral of the product of the source function and $\mathbf{e}^{-\tau_\nu}$

A graphical representation of the integral. Area of the shaded region is the integral.

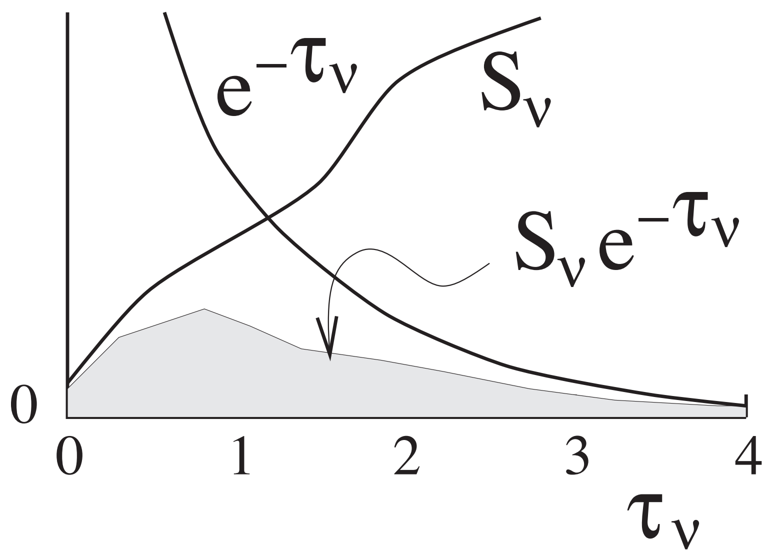

The integral for two different angles: the intensity for the view normal to the surface probes deeper, hotter layers

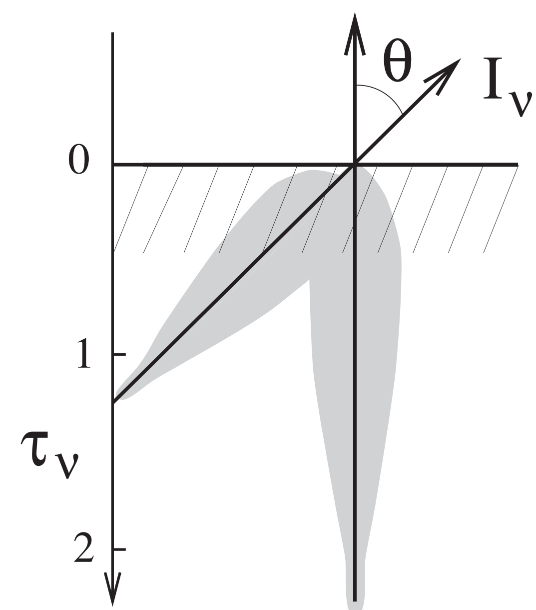

From Rob Rutten's excellent lecture notes:
http://www.phys.uu.nl/~rutten/Astronomy_lecture.html

Limb Darkening Basics III

The *Eddington-Barbier* Approximation

$$I^+_\nu(\tau_\nu\!=\!0,\mu) = \int_0^\infty S_\nu(t_\nu)\,\mathrm{e}^{-t_\nu/\mu}\,\mathrm{d}t_\nu/\mu.$$

$$I^+_\nu(\tau_\nu\!=\!0,\mu) \;\approx\; S_\nu(\tau_\nu=\mu)$$

In the *EB* approximation, the outgoing intensity at a given angle **$\mu=\cos\theta$**, is the source function evaluated at the optical depth **$\tau_\nu = \mu$**.

a) Looking at the disk center: **$I_\nu(\theta=0°) = S_\nu(\tau_\nu = \mu = \cos(0°) = 1) = B_\nu(\tau_\nu = 1)$**

b) Looking toward the limb: **$I_\nu(\theta=60°) = S_\nu(\tau_\nu = \mu = \cos(60°) = ½) = B_\nu(\tau_\nu = ½)$**

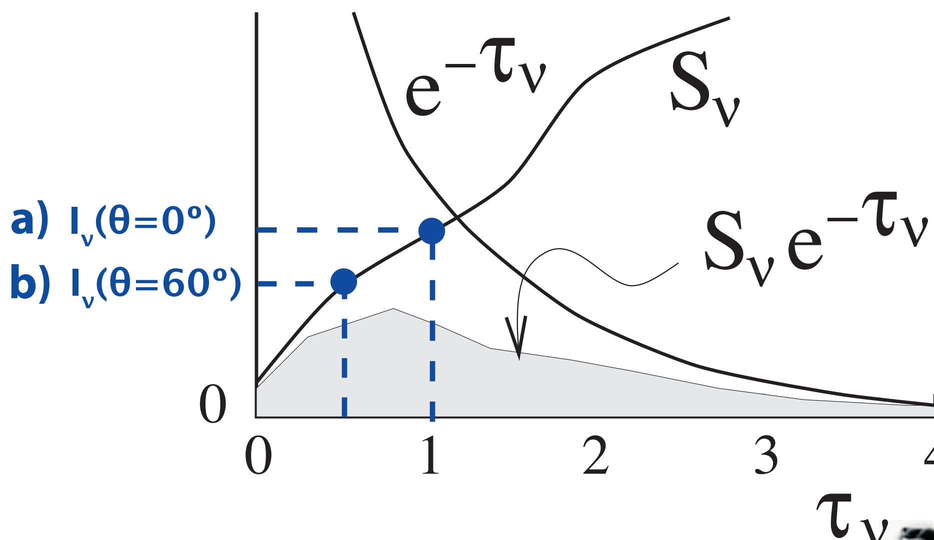

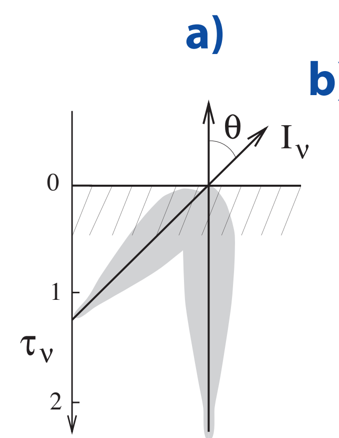

Limb Darkening Basics IV

Continuum wavelength dependence (part II)

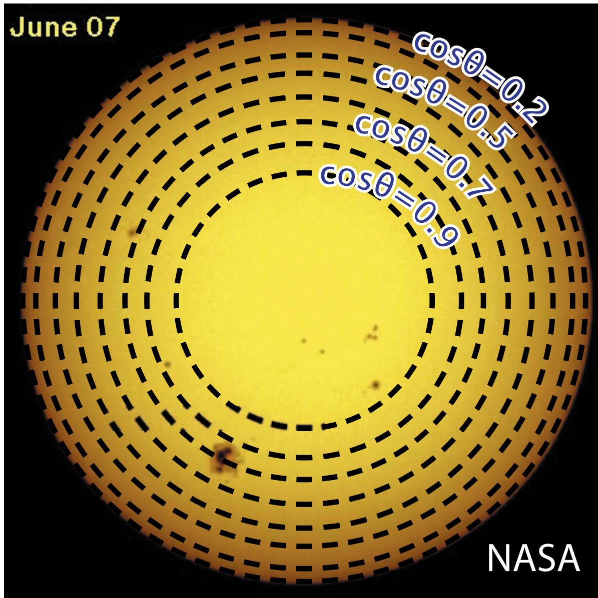

Multiwavelength Limb-darkening Observations

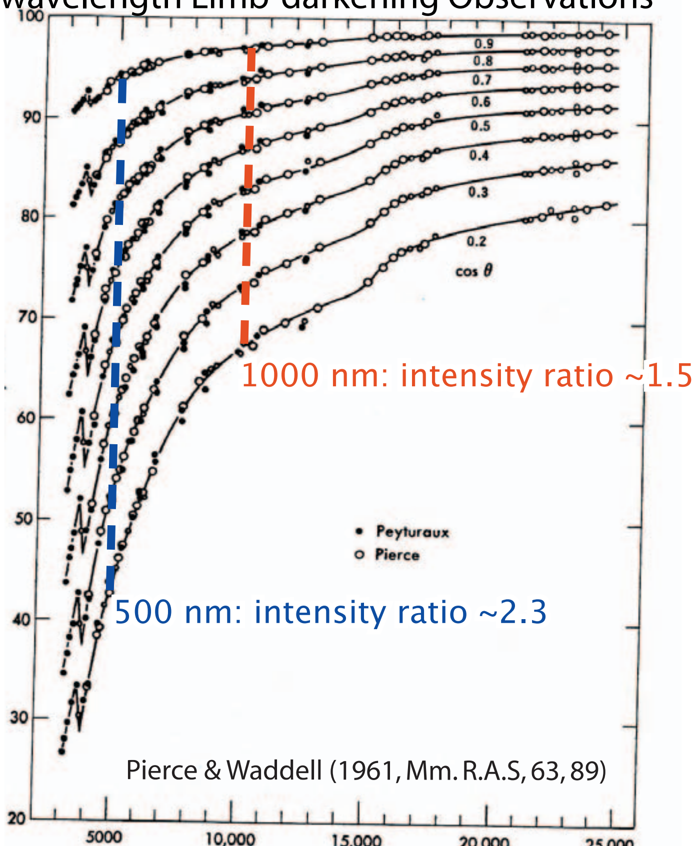

$$\frac{I_\lambda(\tau_\lambda=0,\mu=0.9)}{I_\lambda(\tau_\lambda=0,\mu=0.2)} \approx \frac{B_\lambda(T(\tau_\lambda=0.9))}{B_\lambda(T(\tau_\lambda=0.2))}$$

Eddington Barbier Approximation

$$\tau = \tau_{500\,\mathrm{nm}} \approx \tau_{1000\,\mathrm{nm}}$$

We see to approximately the same physical depths at 500 nm and 1000 nm

$$\frac{I_{500\,\mathrm{nm}}(\mu=0.9)}{I_{500\,\mathrm{nm}}(\mu=0.2)} \approx \frac{B_{500\,\mathrm{nm}}(T(\tau=0.9))}{B_{500\,\mathrm{nm}}(T(\tau=0.2))} = \frac{B_{500\,\mathrm{nm}}(T^{*}=6390\,\mathrm{K})}{B_{500\,\mathrm{nm}}(T=5430\,\mathrm{K})} = 2.23$$

$$\frac{I_{1000\,\mathrm{nm}}(\mu=0.9)}{I_{1000\,\mathrm{nm}}(\mu=0.2)} \approx \frac{B_{1000\,\mathrm{nm}}(T(\tau=0.9))}{B_{1000\,\mathrm{nm}}(T(\tau=0.2))} = \frac{B_{1000\,\mathrm{nm}}(T=6390\,\mathrm{K})}{B_{1000\,\mathrm{nm}}(T=5430\,\mathrm{K})} = 1.55$$

... in good agreement with observations

No surprise, since our Sun's atmospheric temperature structure is derived in part from limb darkening measurements!

*Temperature-optical depth relationship from the Harvard-Smithsonian Reference Atmosphere. See Mihalas "Stellar Atmospheres" (2nd Ed.) page 264.

Solar Limb Darkening and Convection

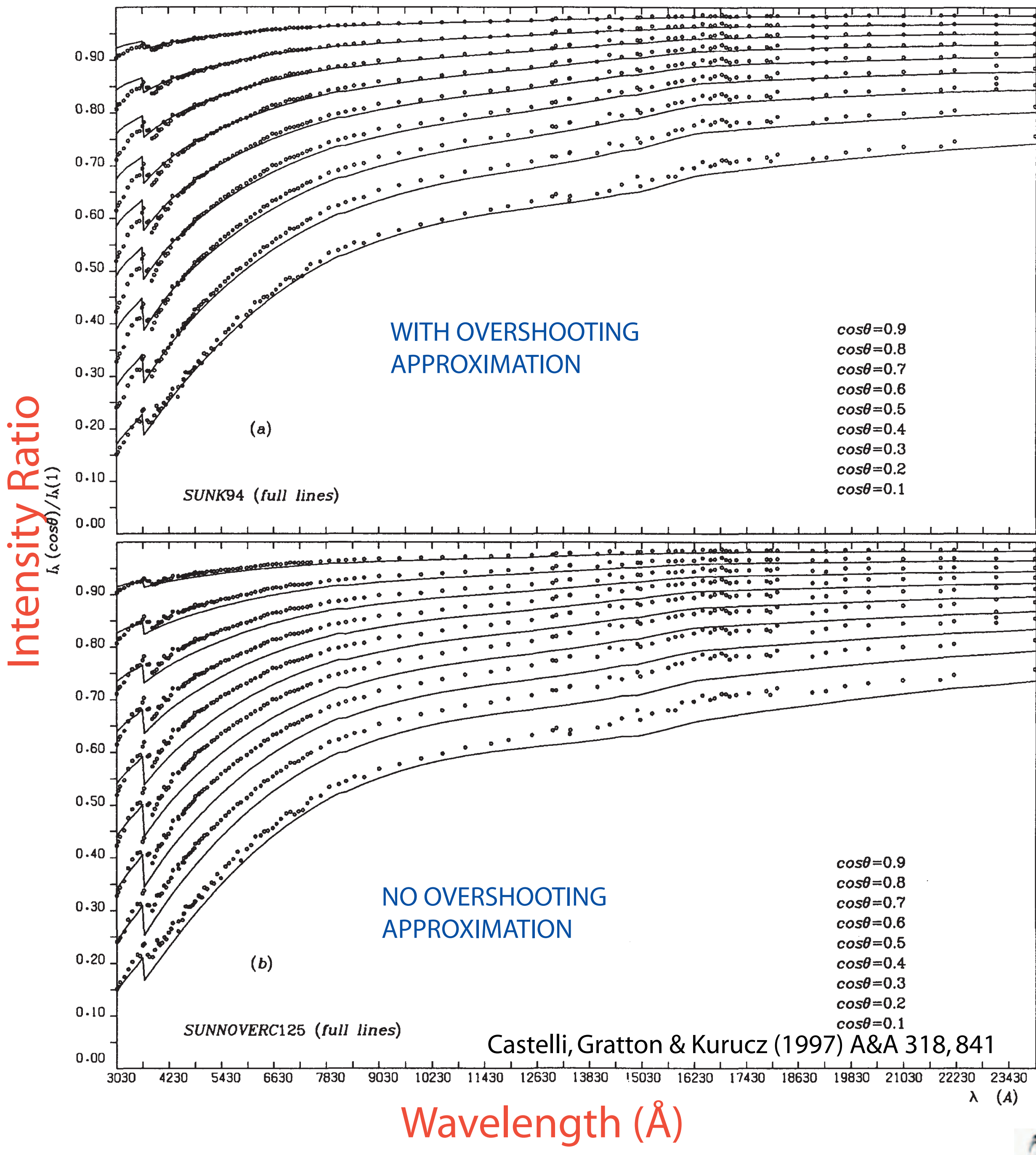

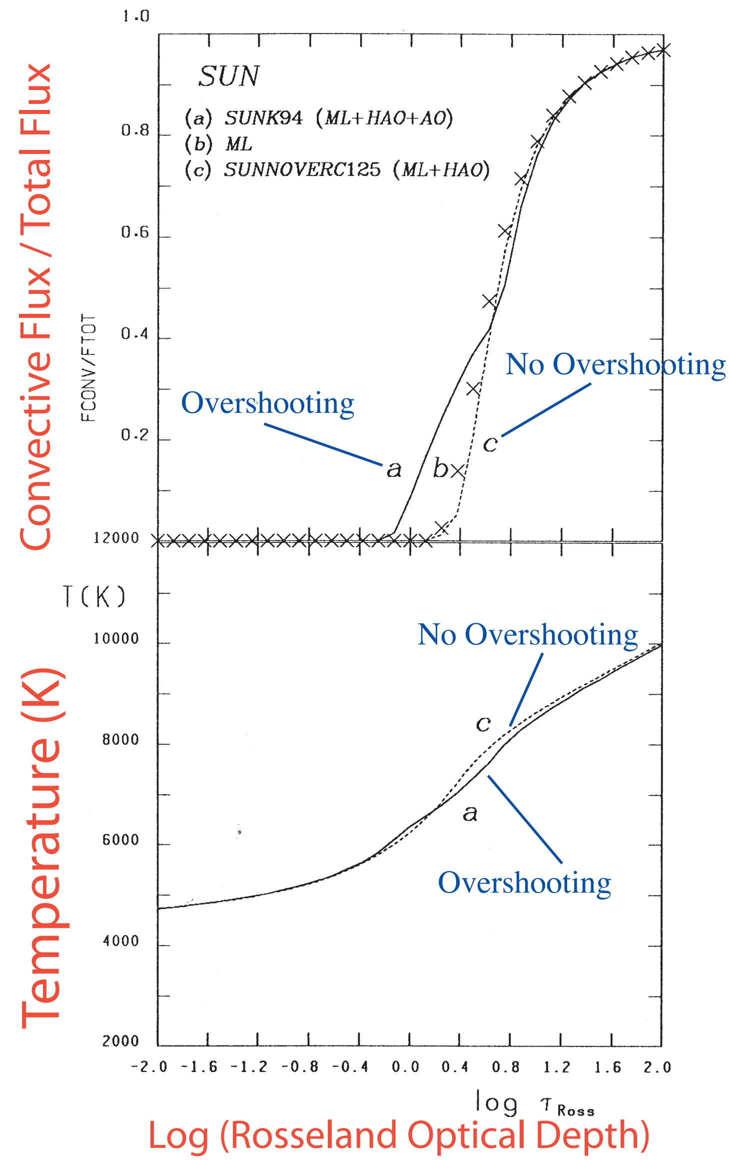

Not So Different from our Sun....

Procyon

Procyon: The Visual Binary (P = 40.82 yr)

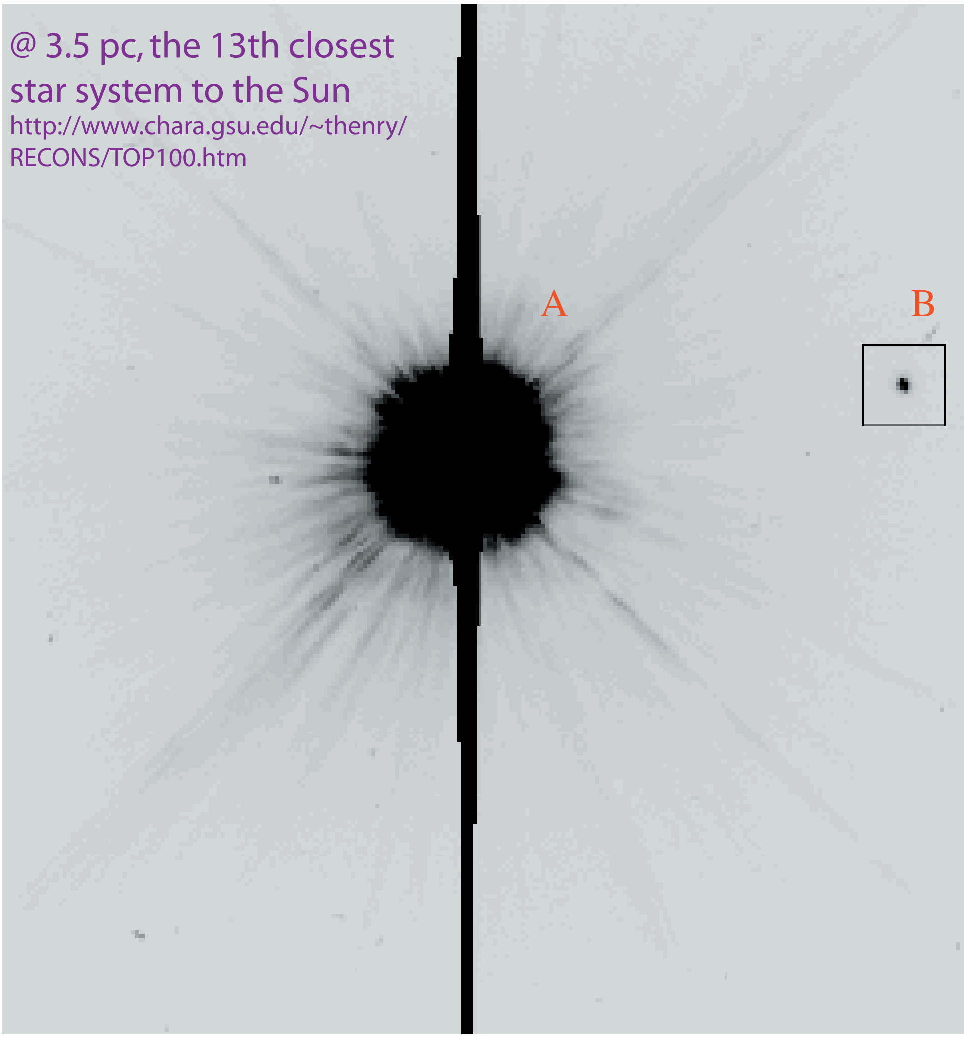

Girard et al (2000) ApJ 119, 2428

HST/WFPC2 PC image (160 s)
F218W filter

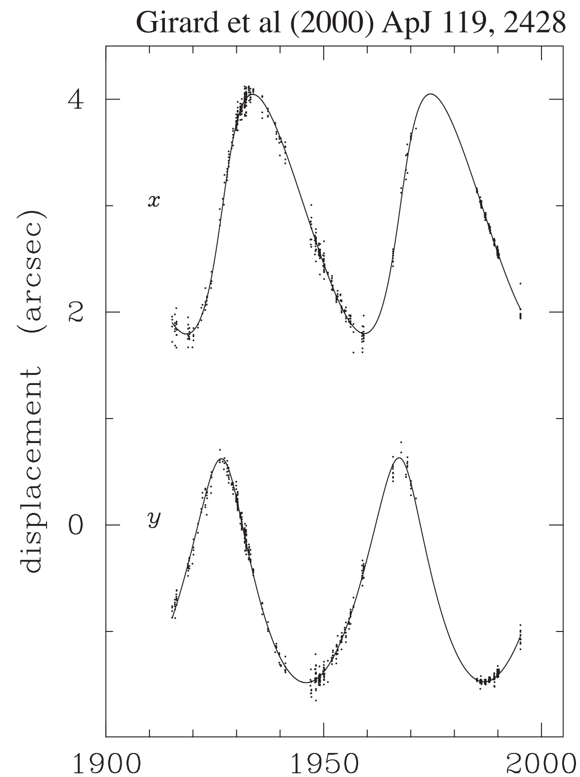

$\text{Mass}_A = 1.497 \pm 0.037\ M_\odot$
$\text{Mass}_B = 0.602 \pm 0.015\ M_\odot$

Procyon A (F5 IV): Fundamental Parameters

Angular diameter = 5.404 $\pm$ 0.03 mas (Kervella et al. 2003)
Parallax = 285.93 $\pm$ 0.88 mas (Hipparcos: Perryman et al.)
Radius = 2.05 $\pm$ 0.02 $R_\odot$
Log(g) = 3.95 $\pm$ 0.02 cgs
Bolometric flux = 17.8 $\pm$ 0.9 x 10^{-9} W m^{-2}
Effective Temperature = 6516 $\pm$ 87 K

3-D and 1-D Model Predictions for Procyon's LD

Granulation Models for Procyon and the Sun

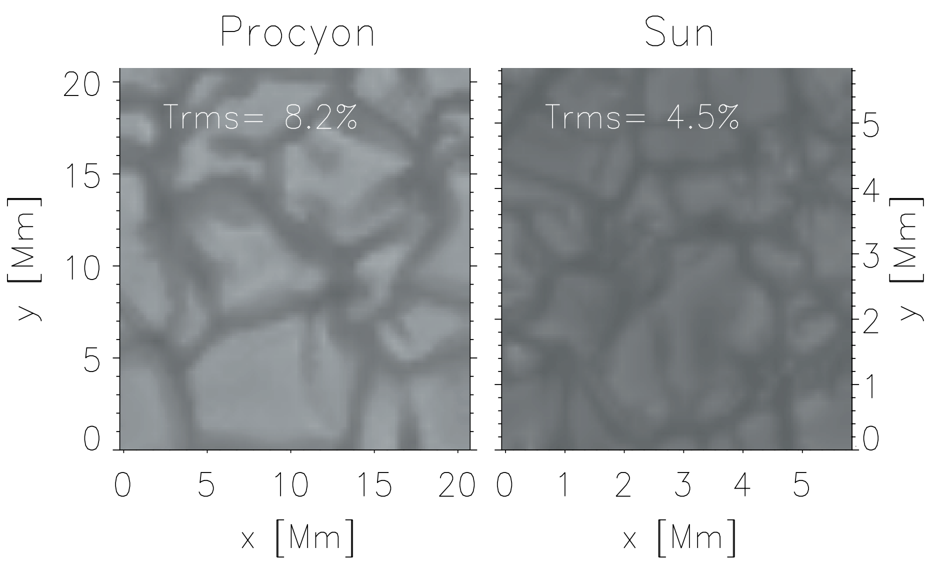

Note: Procyon's temperature RMS (at $\tau = 1$) is 8.2% or 536 K! Compare this to the ±90 K uncertainty in the effective temperature!

3-D versus 1-D Model
Center-to-Limb Profiles for Procyon

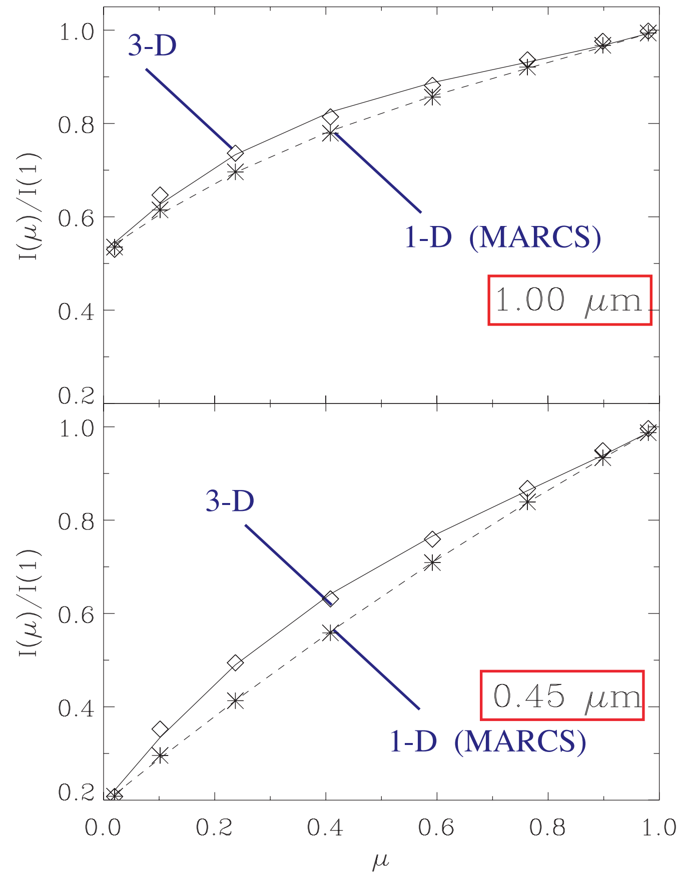

Allende Prieto et al (2002) ApJ 567, 544

3-D Prediction: 1.6 % angular size difference between 1 micron and 450 nm

A 3-D model for Procyon

More Than One Temperature Structure

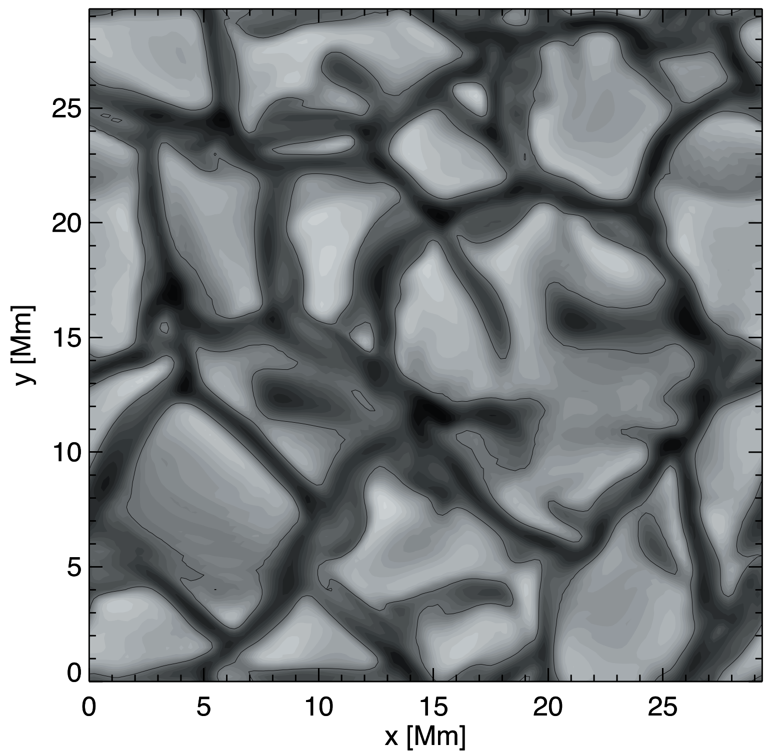

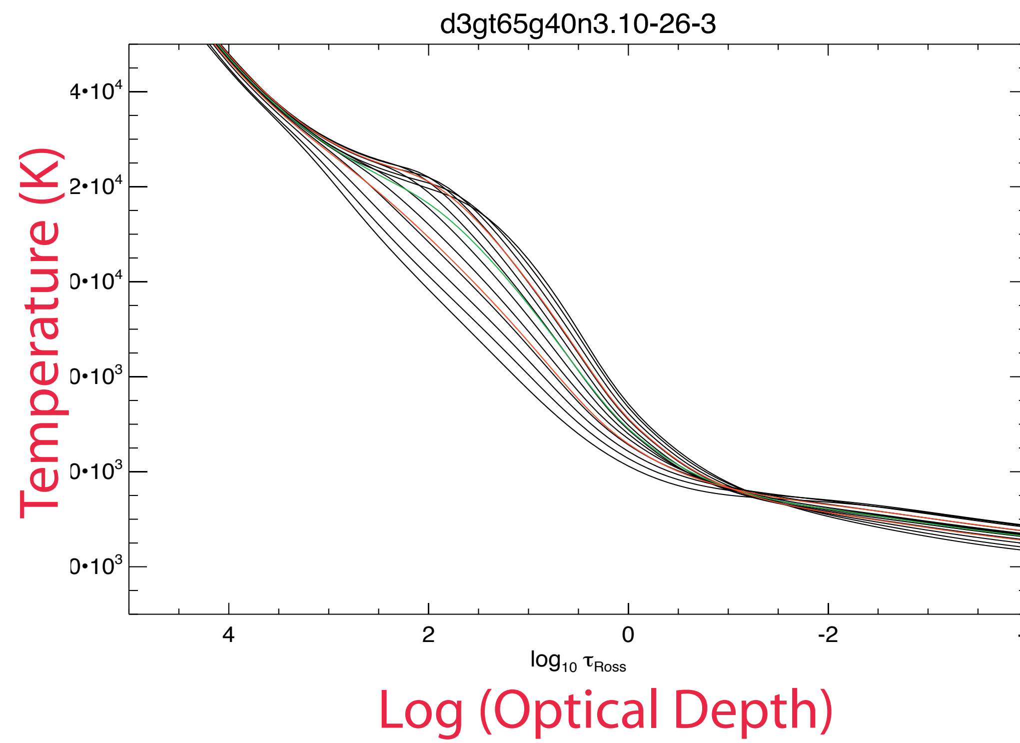

Hotter, rising granules have a warmer temperature structure than cooler, descending dark lanes.

The *mean* 3-D temperature structure differs from a 1-D model and can be detected interferometrically via limb darkening!

A 3-D Models Fits to Procyon at 500 nm, 800 nm, and K-band

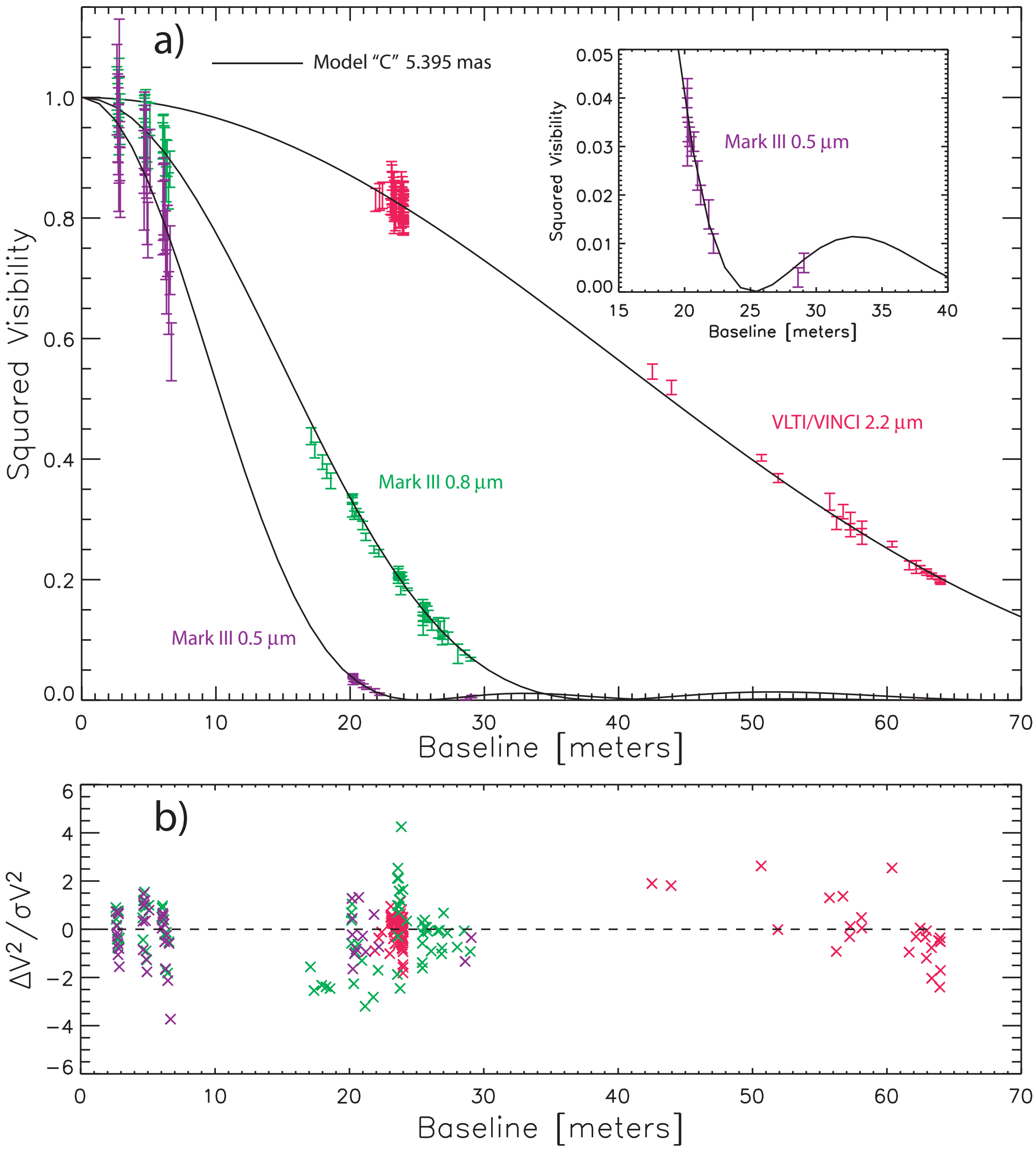

Aufdenberg, Ludwig, Kervella (2005) ApJ 633, 424

Angular Diameters for Procyon from 1-D & 3-D Model Fits

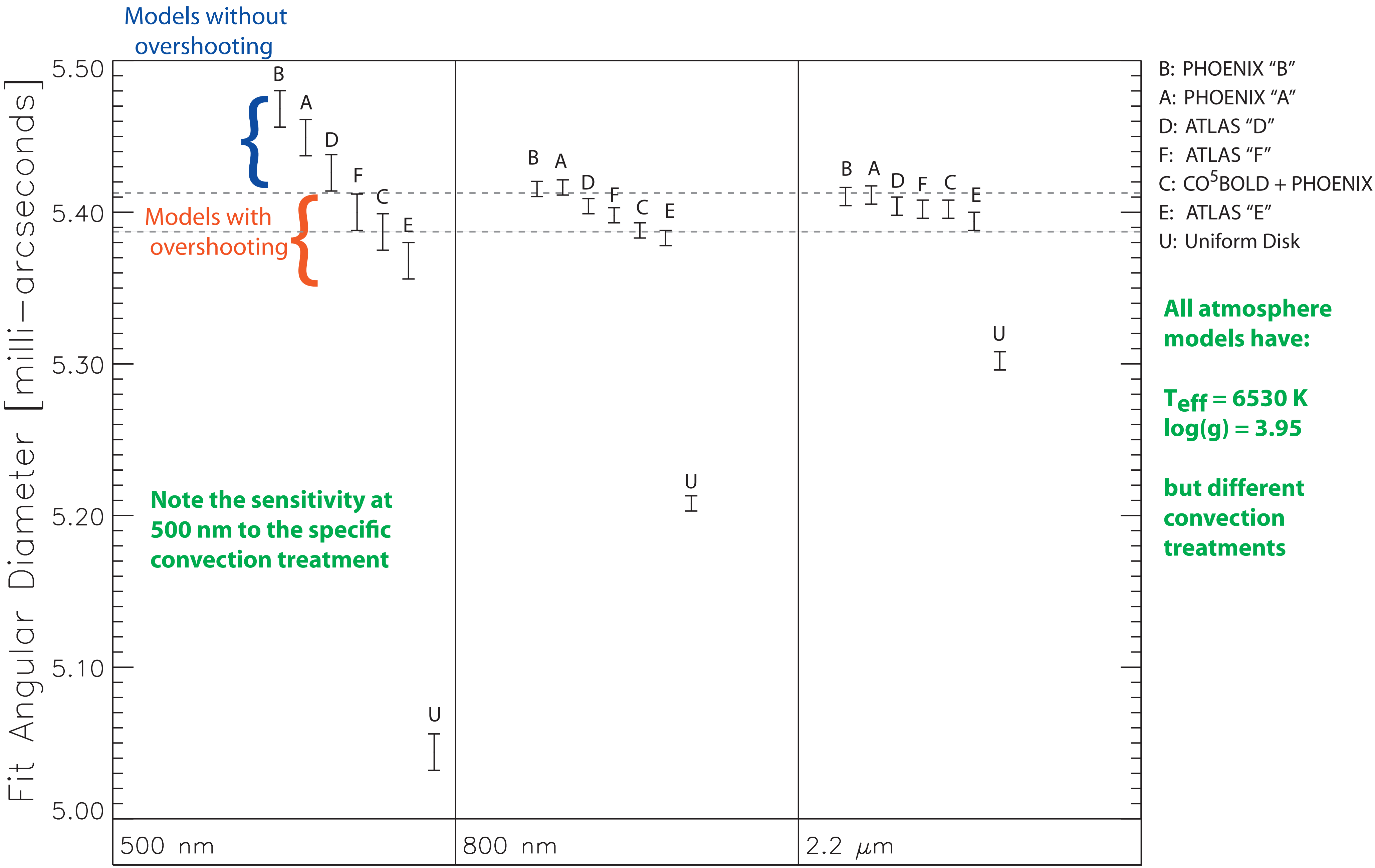

Aufdenberg, Ludwig, Kervella (2005) ApJ 633, 424

Comparing the Corresponding 1-D and 3-D Model Temperature Structures

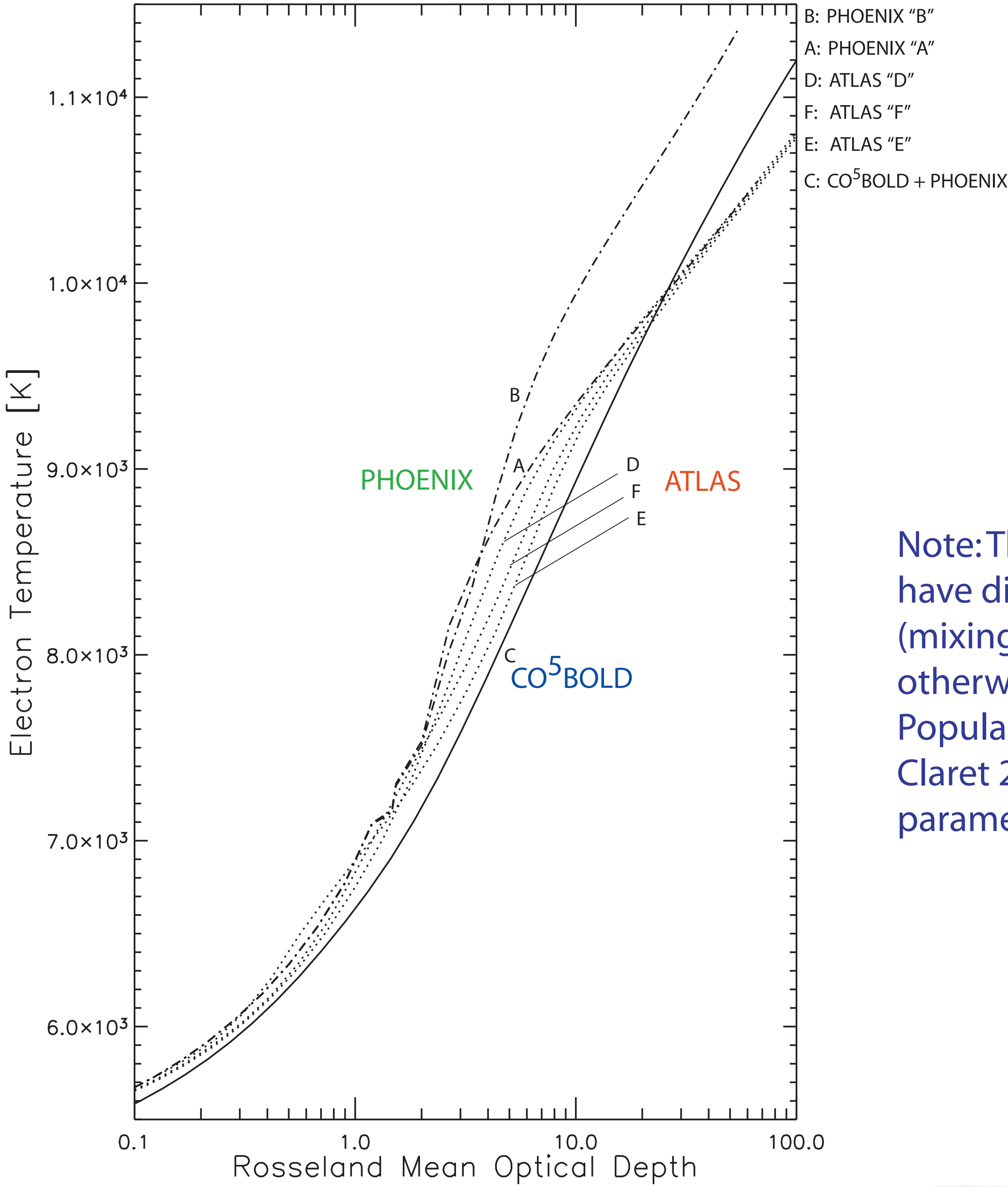

Note: The 3 ATLAS models displayed have different convection treatments (mixing length, overshooting), but otherwise identical stellar parameters. Popular limb darkening tables (e.g. Claret 2004) do not vary convection parameters.

Procyon's Spectral Energy Distribution vs. 1-D and 3-D Stellar Surfaces

3-D Model Surface Intensity Map

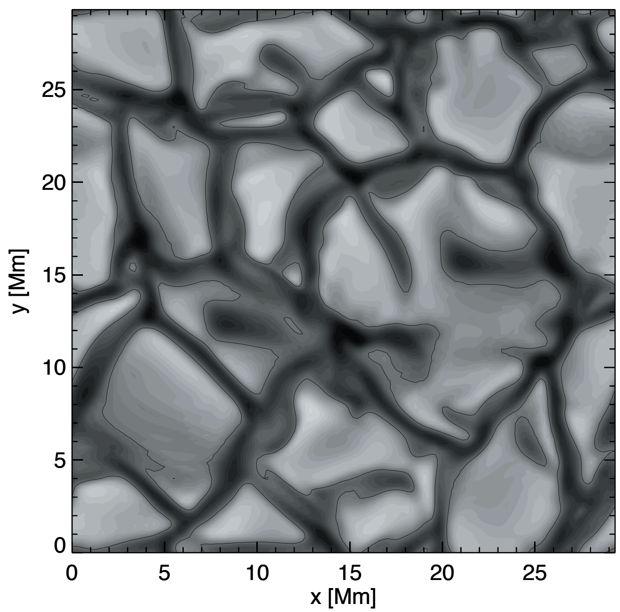

Intensity Histogram

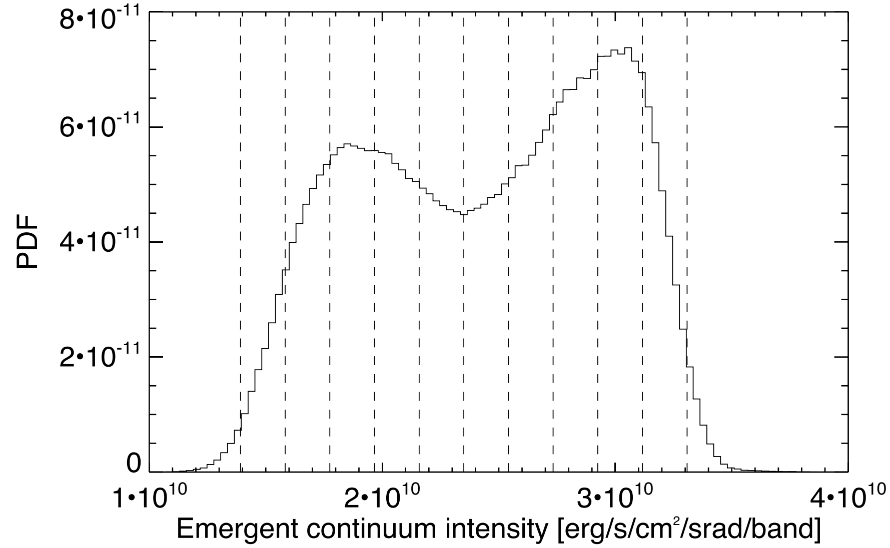

In the ultraviolet, we see only the hot granules, so Procyon's spectrum appears hotter than its effective temperature.

Another check on the 3-D nature of Procyon's atmosphere/surface.

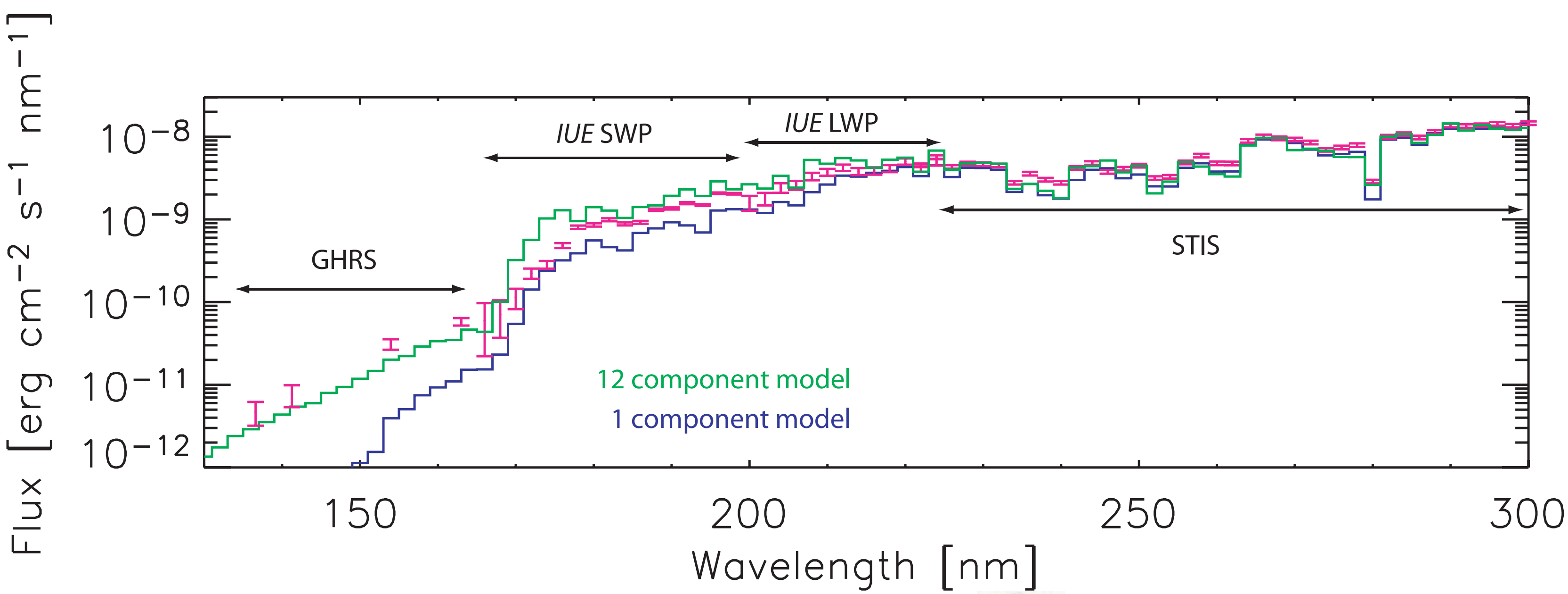

Beyond Plane-Parallel

Spherical Geometry and Atmospheric Extension

•In the examples thus far, the atmospheric thickness was 0.1% of the stellar radius. All effects due to the temperature structure.

•Ordinary extended atmospheres, M giants, have an atmospheric thicknesses of 5% or more.

TiO Bandhead; Narrow Band Filters

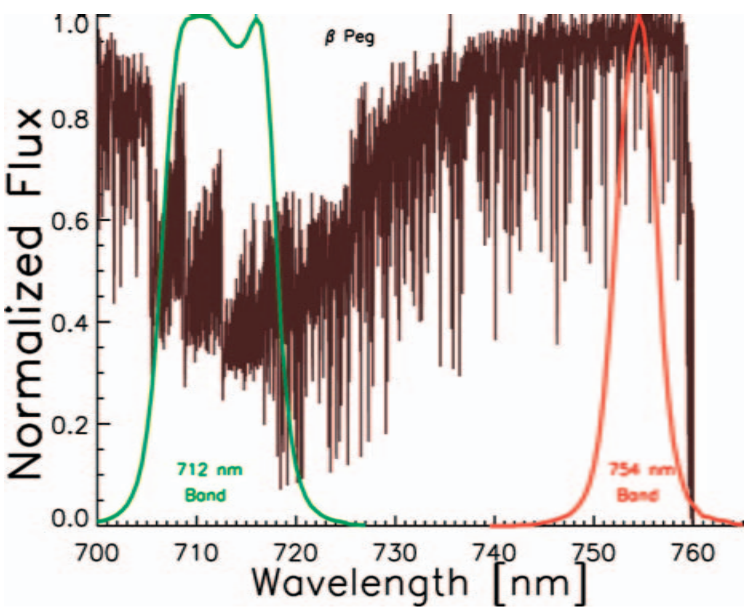

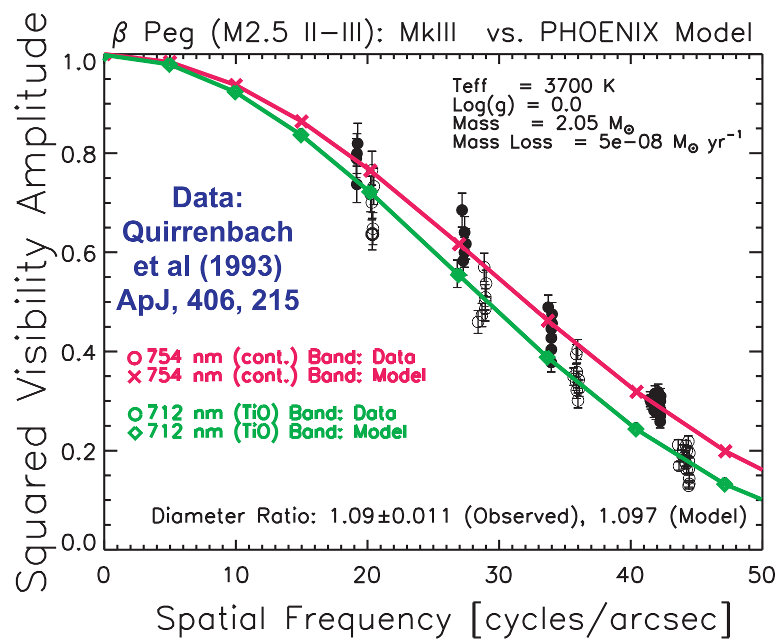

Beyond Plane-Parallel: Spherical Geometry and Atmospheric Extension

How "fuzzy" is the limb of a star?

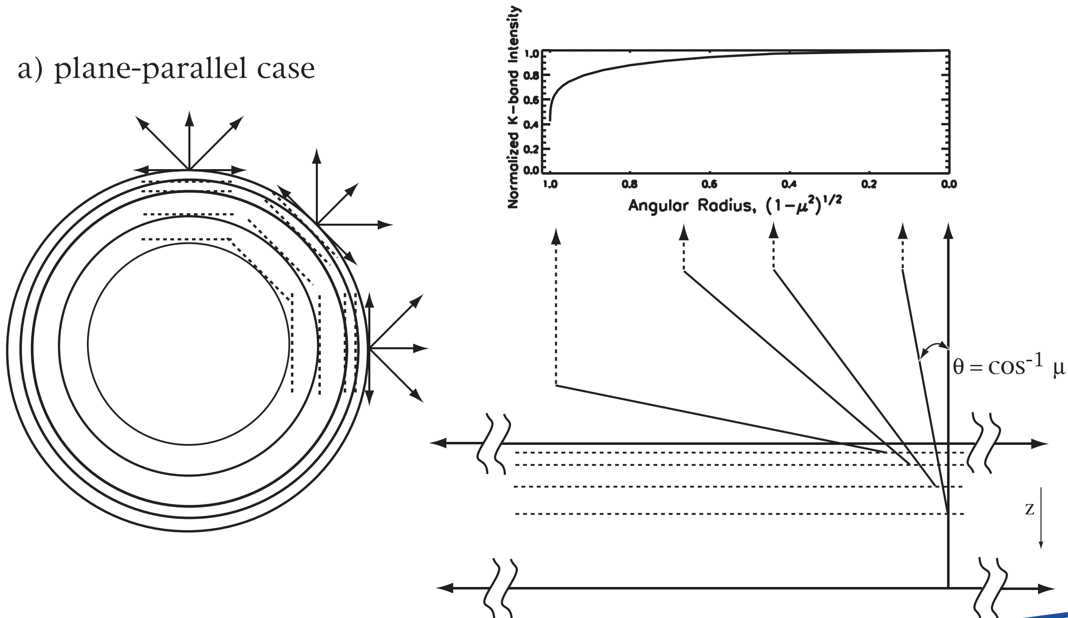

The semi-infinite nature of plane-parallel models means that the atmosphere is optically thick at all angles.

Drop off characteristic of spherical models.

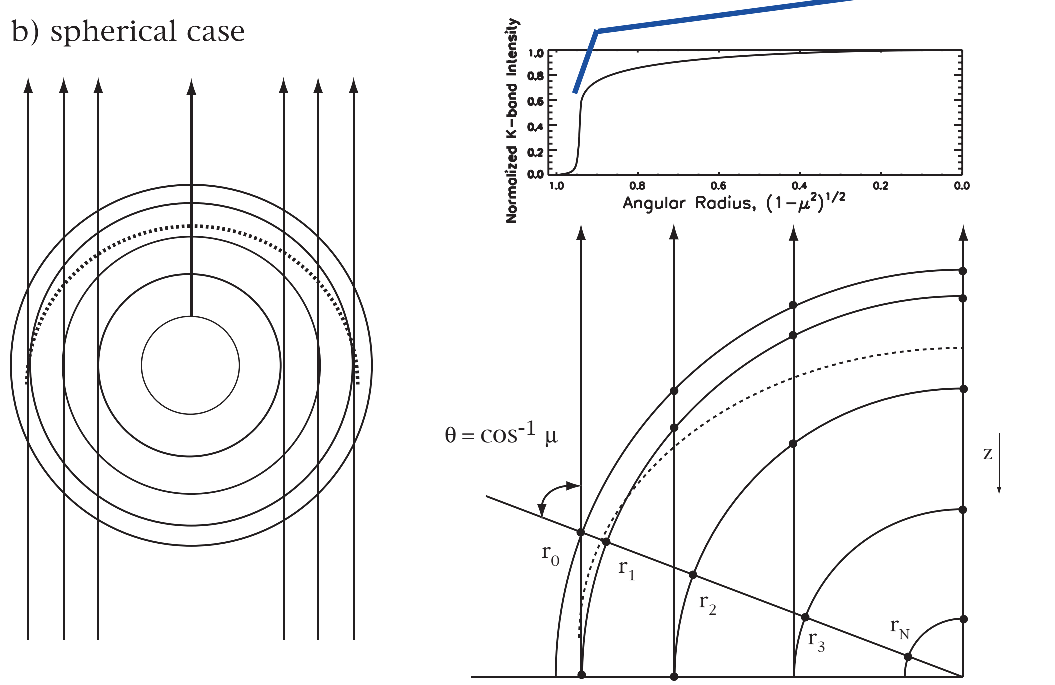

The rays of a spherical model impact nested shells, of which the outer most are optically thin.

Spherical Models and Multi-Wavelength Data: The Case of γ Sge (M0 III)

Spherical Model Yields Consistent Diameter Across Optical/Near-IR

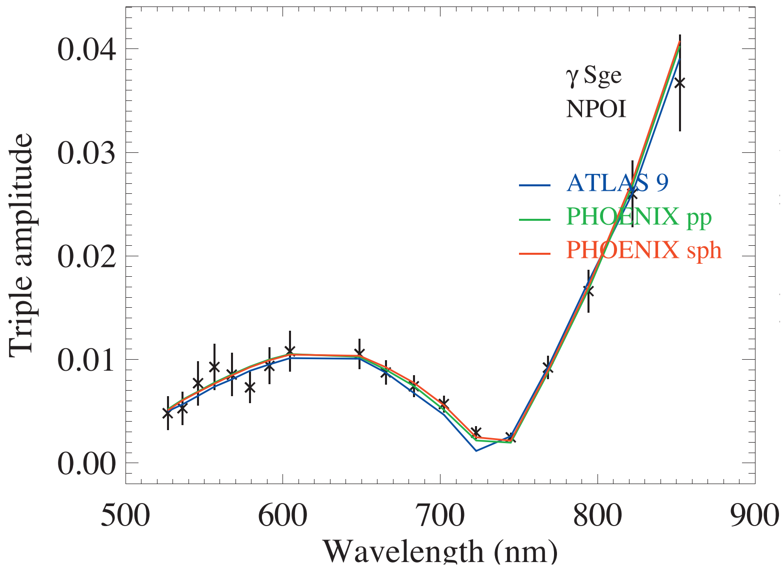

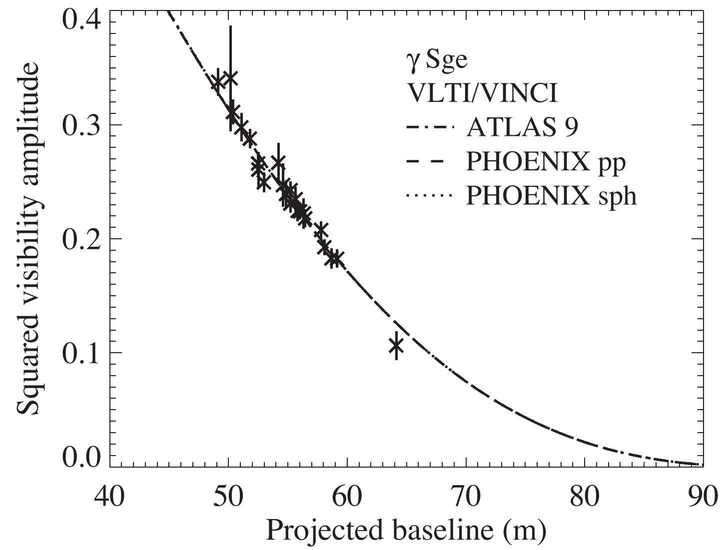

Table 5. Results for the fit of ATLAS 9 and PHOENIX model atmospheres to our interferometric VLTI/VINCI and NPOI data sets of γ Sagittae.

Model atmosphere	NPOI (526 nm to 852 nm)	VLTI/VINCI (2190 nm)
ATLAS 9, plane-parallel, $T_{\rm eff}$ = 3750 K, log g = 1.0	$\Theta_{\rm LD}$ = 6.18 ± 0.06 mas χ^2_ν = 2.2	$\Theta_{\rm LD}$ = 6.05 ± 0.02 mas χ^2_ν = 0.6
PHOENIX, plane-parallel, $T_{\rm eff}$ = 3750 K, log g = 1.0	$\Theta_{\rm LD}$ = 6.11 ± 0.06 mas χ^2_ν = 2.3	$\Theta_{\rm LD}$ = 6.05 ± 0.02 mas χ^2_ν = 0.6
PHOENIX, spherical, $T_{\rm eff}$ = 3750 K, log g = 1.0, $M = 1.3\,M_\odot$	$\Theta_{\rm LD}$ = 6.30 ± 0.06 mas χ^2_ν = 2.4 $\Theta_{\rm Ross}$ = 6.02 ± 0.06 mas	$\Theta_{\rm LD}$ = 6.30 ± 0.02 mas χ^2_ν = 0.6 $\Theta_{\rm Ross}$ = 6.02 ± 0.02 mas

All atmosphere models have: $T_{\rm eff}$ = 3750 K, log(g) = 1.0
but different geometries

Wittkowski et al. (2006a) A&A, submitted

Spherical Geometry: More Parameters, More Model-Dependent Results

Spherical Models are parameterized by:

T_{eff}, log(g), Mass or Radius

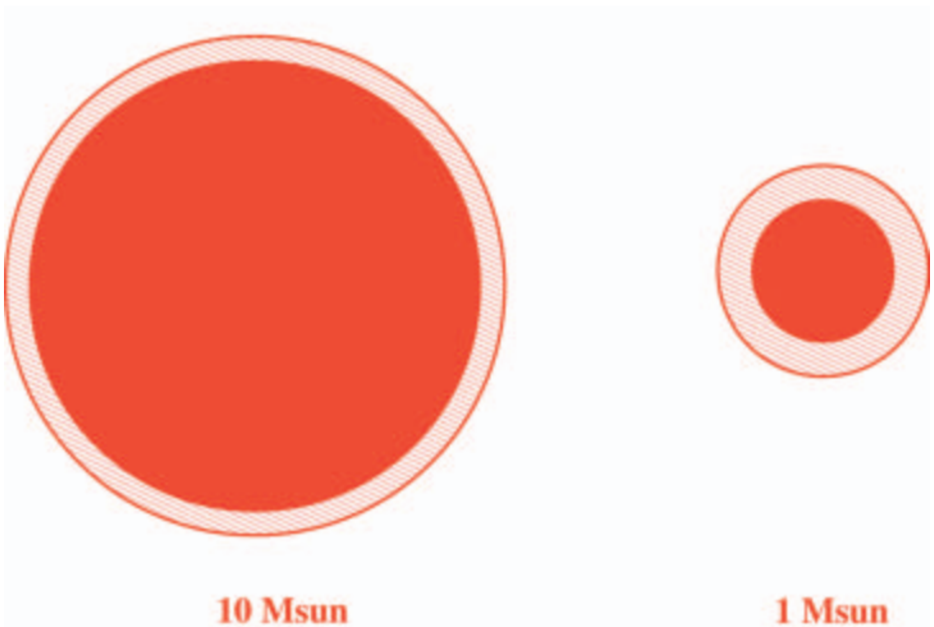

Two stars:

same T_{eff} & log(g), different Mass

$$T_{eff} = \left[\frac{4\mathcal{F}_0}{\sigma\theta^2_{LD}}\right]^{1/4}$$

Angular Diameter (corrected for limb darkening)

Bolometric Flux (corrected for extinction)

follows from:

$$4\pi d^2 \mathcal{F}_0 = L = 4\pi R^2 \sigma T^4_{eff}$$

distance — luminosity — radius

$$\mathcal{F}_0 = \frac{R^2}{d^2}\sigma T^4_{eff}$$

$$\mathcal{F}_0 = \frac{\theta^2}{4}\sigma T^4_{eff}$$

T_{eff} is not well-defined in a spherical atmosphere , so a *reference radius* must be chosen.

One such radius: the *Rosseland Radius*.

Spherical Models and the Rosseland Diameter

Rosseland Radius: Radius at which τ_R is unity

$$\mathrm{d}\tau_\mathrm{R} = -\kappa_\mathrm{R}\rho\,\mathrm{d}z \qquad \int_0^\infty \frac{1}{\kappa_\nu}\frac{\mathrm{d}B_\nu/\mathrm{d}T}{\mathrm{d}B/\mathrm{d}T}\,\mathrm{d}\nu \equiv \frac{1}{\kappa_\mathrm{R}}$$

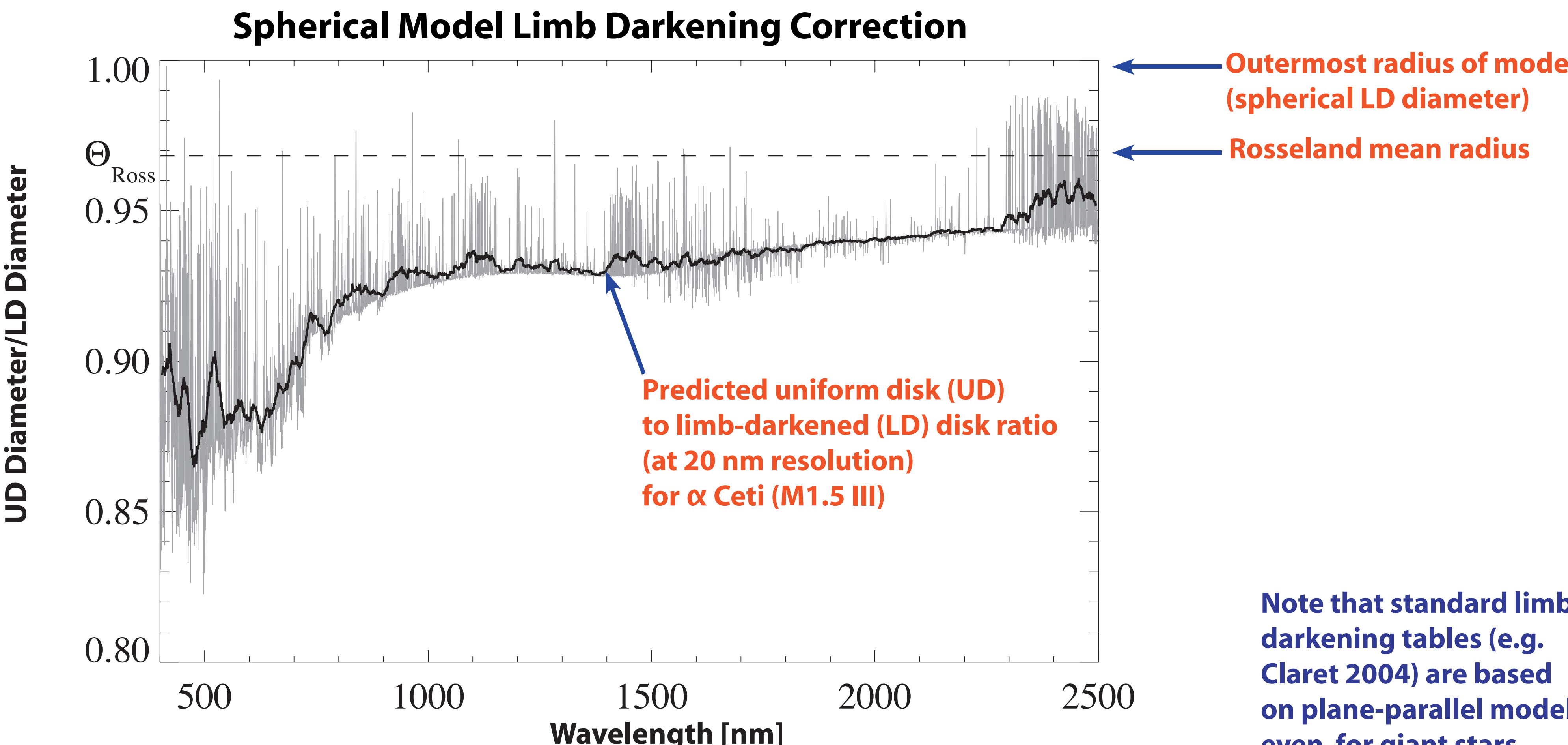

Note that standard limb darkening tables (e.g. Claret 2004) are based on plane-parallel models, even for giant stars

See Mihalas "Stellar Atmospheres" (2nd Ed.), sec. 3-2.   Wittkowski et al. (2006b) A&A, submitted

Odds and Ends

Limb Darkening vs. Gravity Darkening

Rapidly Rotating Model with Intensity Contours

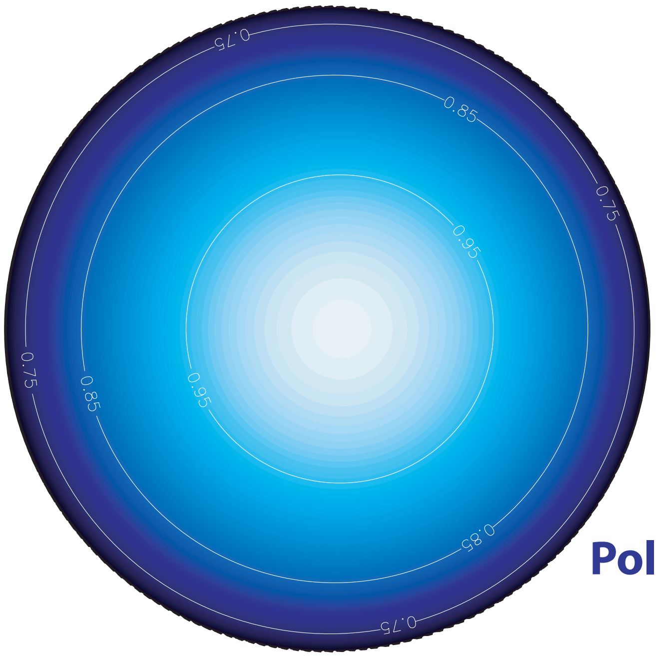

Pole-on view

Gravity darkening: *Intrinsic to the star, a pole-to-equator effective temperature gradient resulting from rapid rotation. Local Teff on surface correlates with local gravity (e.g., $T_{eff} \propto g^{1/4}$)*

Limb darkening: *An observer-dependent effect in which the intensity across a stellar surface varies due to a radial or depth-dependent temperature gradient.*

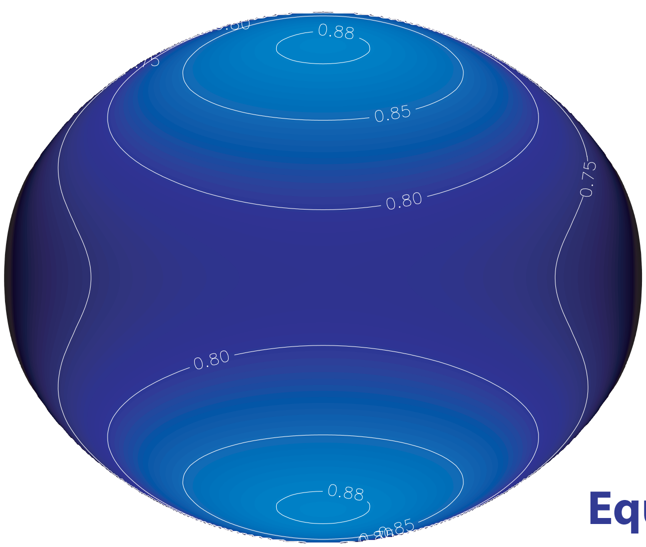

Equator-on view

Note: In the equator-on view, the hottest region (the pole) is also the most limb darkened.

Therefore, the brightest patch of the equator-on view is slightly below the pole and fainter by ~10%

Aufdenberg et al. (2006) ApJ, 645, 664

Stars Are Not Blackbodies

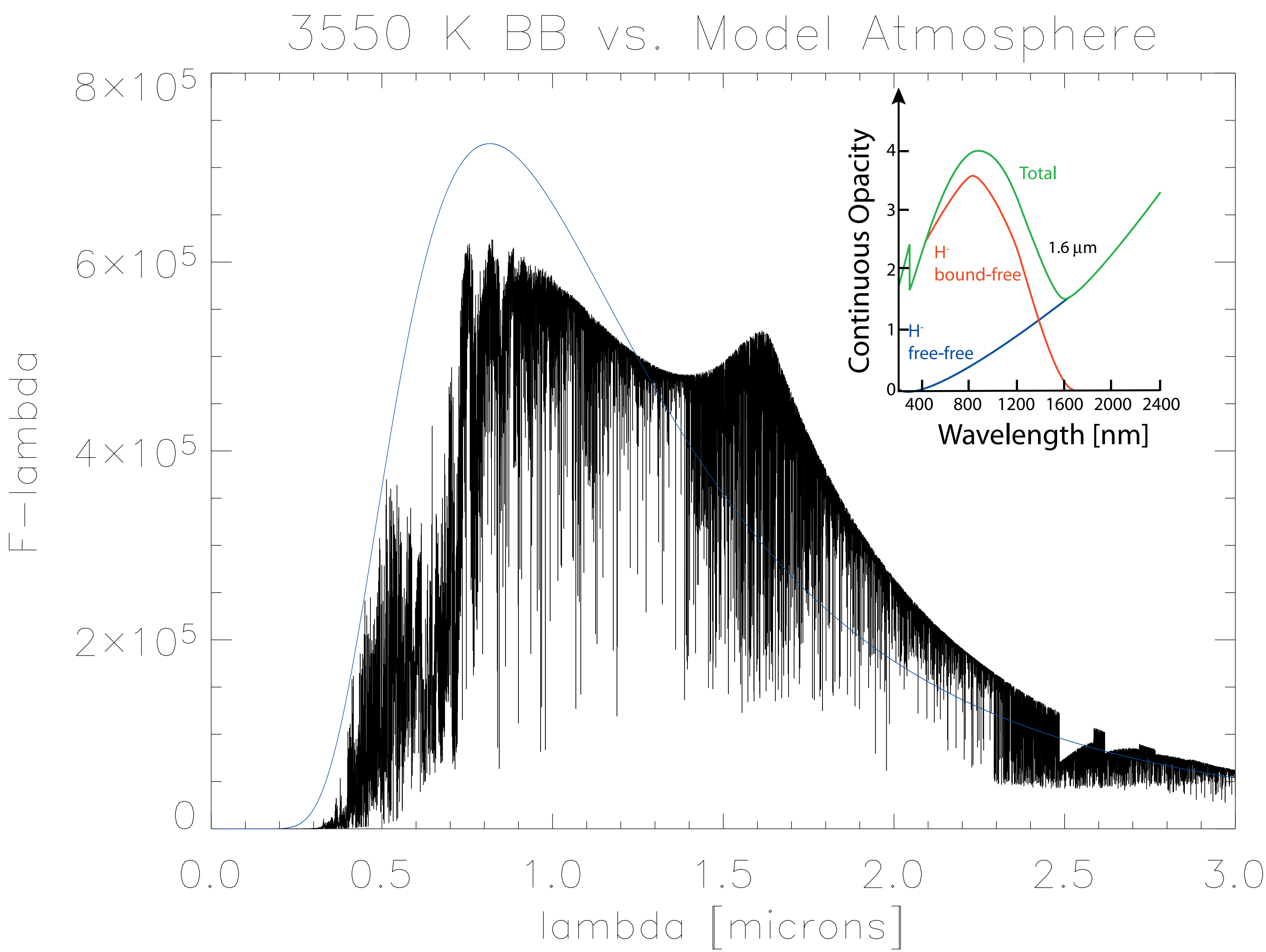

Synthetic Visibilities in 2-D (for stars lacking azimuthal symmetry)

$$V_\lambda^2(u,v) = \left[\int_{-\infty}^{\infty}\int_{-\infty}^{\infty} S_\lambda I_\lambda(x,y) e^{i2\pi(u\,x+v\,y)}\,\mathrm{d}x\,\mathrm{d}y\right]^2$$

$$V_k^2(u_k,v_k) \approx \left[\sum_{i=1}^{N} A_i \sum_{j=1}^{N} A_j S_k I_k(x_i,y_j)\cos(2\pi(u_k x_i + v_k y_j))\right]^2 + \left[\sum_{i=1}^{N} A_i \sum_{j=1}^{N} A_j S_k I_k(x_i,y_j)\sin(2\pi(u_k x_i + v_k y_j))\right]^2$$

$$V_k^2(0,0) \approx \left[\sum_{i=1}^{N} A_i \sum_{j=1}^{N} A_j S_k I_k(x_i,y_j)\right]^2.$$

$$V(B,\lambda_0)^2 = \frac{\int_0^\infty V(B,\lambda)^2\,\lambda^2\,\mathrm{d}\lambda}{\int_0^\infty V(0,\lambda)^2\,\lambda^2\,\mathrm{d}\lambda}.$$

$$\lambda_0^{-1} = \frac{\int_0^\infty \lambda^{-1}\ S(\lambda)\ F_\lambda\ \mathrm{d}\lambda}{\int_0^\infty S(\lambda)\ F_\lambda\ \mathrm{d}\lambda},$$

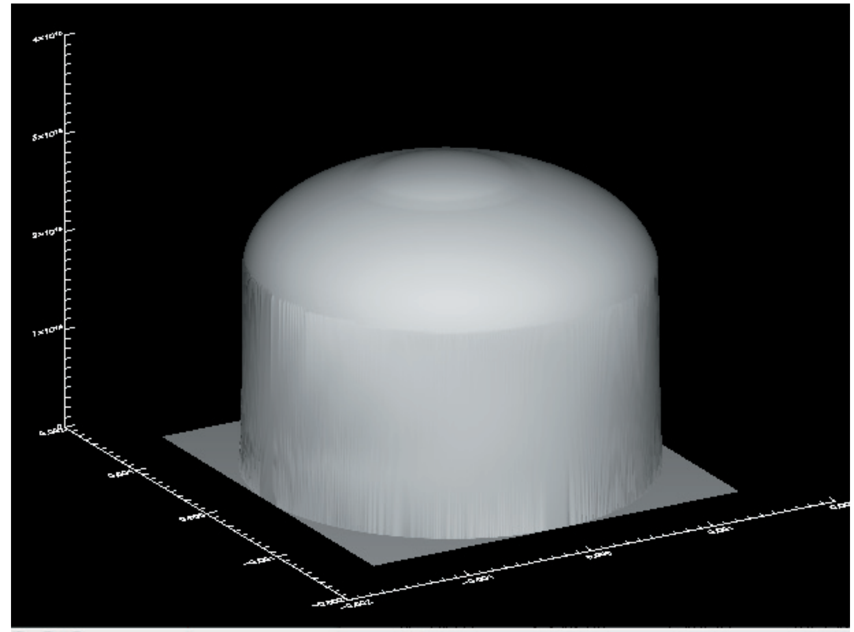

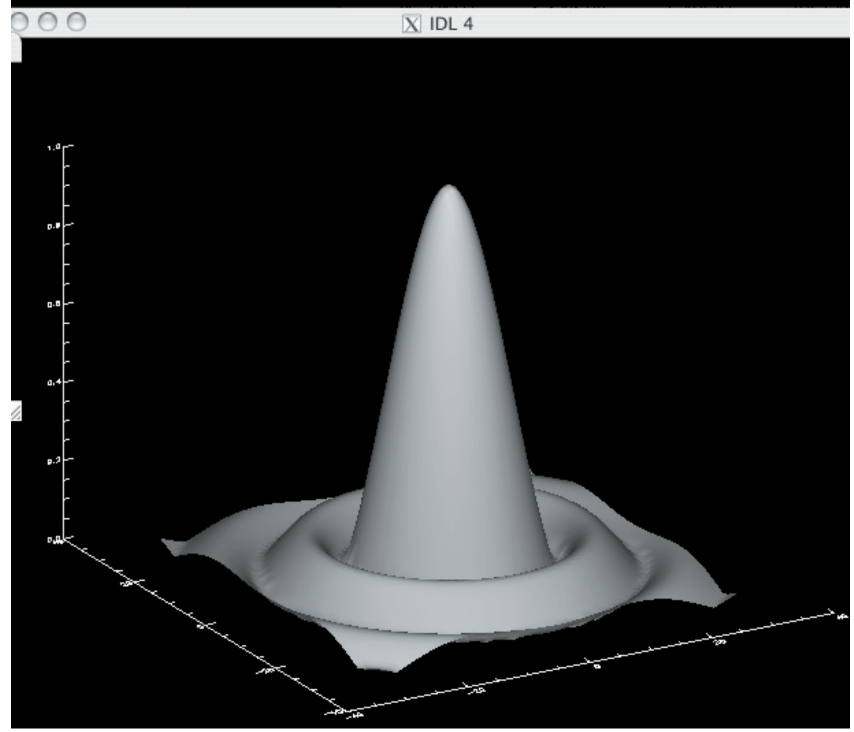

For details please see Aufdenberg et al. (2006) ApJ, 645, 664

Interesting Stellar Surfaces for the Future

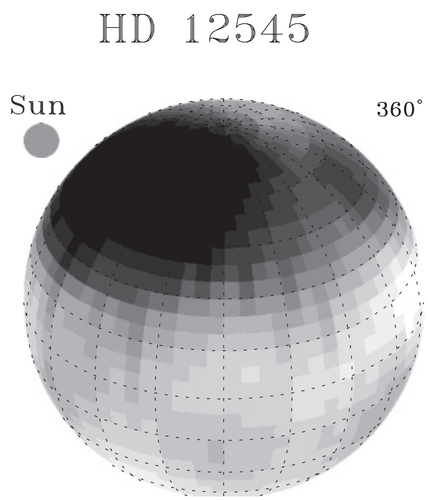

Super starspots via Doppler Imaging
Strassmeier et al. (1999) A&A 347 225

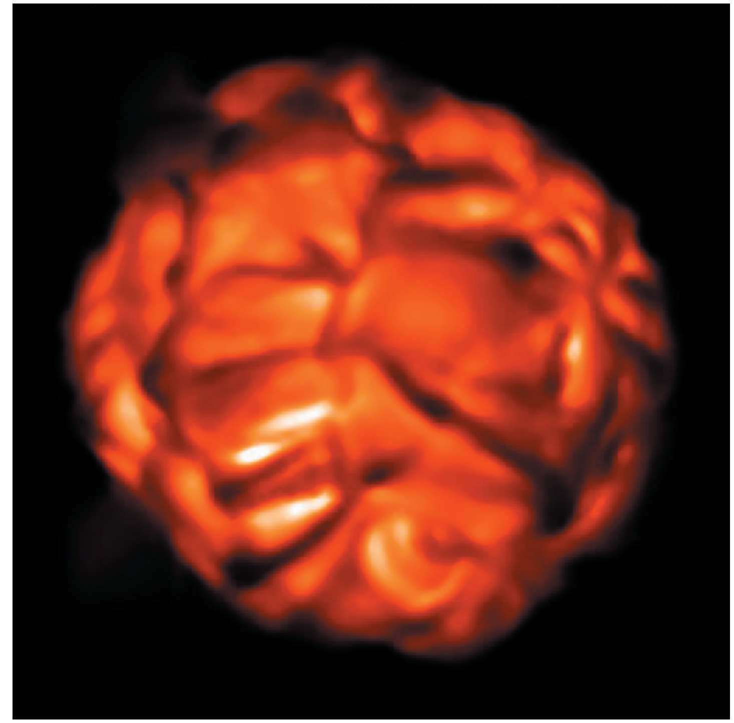

Betelgeuse model by Bernd Freytag

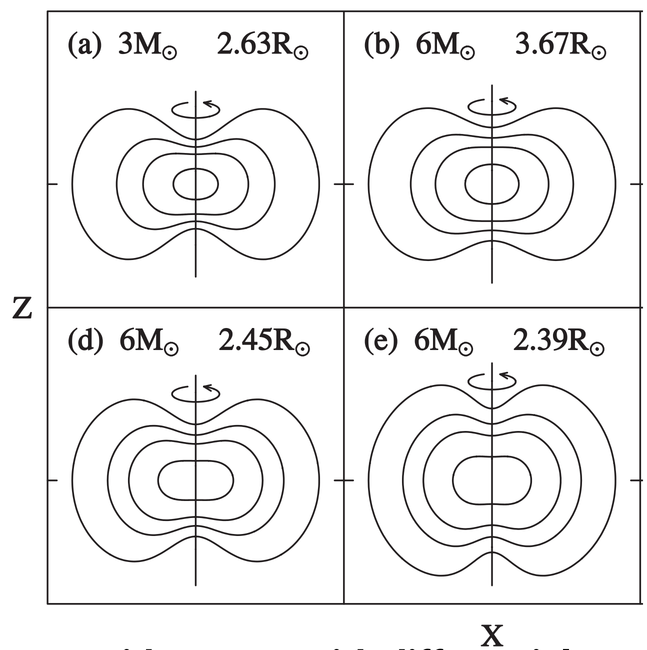

Rapid rotators with differential rotation
Jackson et al. (2005) ApJS 156, 245

Summary

High-precision interferometry allows us study fundamental aspects of stellar structure.

Even geometrically thin atmospheres have subtle effects (convection!) that can be probed. Standard limb-darkening tables don’t include this, be careful.

Multi-wavelength observations are crucial for studying stellar structure.

In the blue, observations are more sensitive to stellar structure: $\partial B_\lambda/\partial T$ rules!

Spherical models required for consistent, high-precision diameters of giants.

Many fascinating stellar surfaces waiting to be imaged interferometrically.
Here’s to closure phases!

Questions Please!

Michelson Summer School 2003 slides here: http://msc.caltech.edu/workshop/2003/2003_MSS/10_Thursday/aufdenberg.pdf